Title

Modeling of thermally driven hydrological processes in partially saturated fractured rock

Author

Tsang, Yvonne

Publication Date

2010-02-02

Modeling of Thermally Driven Hydrological Processes in Partially Saturated Fractured Rock

Y. W. Tsang, J. T. Birkholzer, and S. Mukhopadhyay

Earth Sciences Division

Lawrence Berkeley National Laboratory

University of California

Berkeley, California, U. S. A.

ABSTRACT

This paper is a review of the research that led to an in-depth understanding of flow and transport processes under strong heat stimulation in fractured, porous rock. It first describes the anticipated multiple processes that come into play in a partially saturated, fractured porous volcanic tuff geological formation, when it is subject to a heat source such as that originating from the decay of radionuclides. The rationale is then given for numerical modeling being a key element in the study of multiple processes that are coupled. The paper outlines how the conceptualization and the numerical modeling of the problem evolved, progressing from the simplified to the more realistic. Examples of numerical models are presented so as to illustrate the advancement and maturation of the research over the last two decades. The most recent model applied to *in situ* field thermal tests is characterized by (1) incorporation of a full set of thermal-hydrological processes into a numerical simulator, (2) realistic representation of the field test geometry, in three dimensions, and (3) use of site-specific characterization data for model inputs. Model predictions were carried out prior to initiation of data collection, and the model results were compared to diverse sets of measurements. The approach of close integration between modeling and field measurements has yielded a better understanding of how coupled thermal hydrological processes produce redistribution of moisture within the rock, which affects local permeability values and subsequently the flow of liquid and gases. The fluid flow in turn will change the temperature field. We end with a note on future research opportunities, specifically those incorporating chemical, mechanical, and microbiological factors into the study of thermal and hydrological processes.

INTRODUCTION AND BACKGROUND

The containment of spent fuel from nuclear power plants in a geological repository is the nuclear-waste-disposal option of choice for many countries worldwide. As early as 1957, a United States National Academy of Sciences report [*NAS*, 1957] recommended burying radioactive waste in geological formations. Similar panel studies in other countries have given rise to a consensus worldwide that deep geological disposal is the scientifically credible long-term solution for managing high-level radioactive waste.

Radioactive decay of high-level nuclear waste releases heat that will increase the temperature of rock surrounding a geological repository. This gives rise to coupled processes that are primarily thermal-hydrological, thermal-hydrologic-chemical, and thermal-hydrologic-mechanical in nature. These coupled processes are key elements in the safety assessment of a high-level radioactive waste repository, because they impact the possible transport of radionuclides (some having very long half-lives—10^4 to 10^6 years) in the rock formation to the biosphere, should the radionuclides escape the waste canisters intended to contain them. A fundamental understanding of these coupled processes, including the ability to model and predict (with confidence) their effects over periods of time unprecedented in science and engineering, is essential for demonstrating the effective geologic isolation of nuclear waste.

In 1985, international agencies convened a symposium on coupled processes affecting the performance of a nuclear waste repository [*Tsang*, 1987]. In the ensuing decades, the quest for safe geological disposal of radioactive waste has greatly highlighted the importance of coupled processes in geosciences research. While conceptual models and numerical simulations (the subject matter of this review) are essential for understanding coupled processes in geological formations, another key component of coupled processes research involves *in situ* tests, which the international nuclear-waste research community has pursued aggressively. The following is a list of field thermal tests conducted in waste-disposal programs around the world:

1) Full-scale and time-scale heater tests in granite in the Stripa iron mines of Sweden [*Cook and Hood*, 1978; *Cook and Witherspoon*, 1978; *Robinson*, 1985; *Witherspoon*, 2000];
2) A heater test in granite at Fanay Augéres, France [*Rejeb et al*., 1993];
3) The CACTUS (ChAracterization of Clay under Thermal loading for Underground Storage) [*Picard et al.*, 1991; 1995] and CERBERUS (Control Experiment with Radiation of the BElgian Repository for Underground Storage) [*Noynaert et al*., 1995] tests at the Mol Underground Laboratory in Belgium;
4) A heater test in granidiorite at the Kamaishi mine in Japan [*Chijimatsu et al.,* 2001];
5) The Grimsel heater test [Lieb, 1988] and FEBEX (Full-scale Engineered Barriers EXperiment) test in granitic crystalline rock within Switzerland's underground laboratory [*Alonso and Alcoverro*, 2003];
6) A heater test series in a granite pluton at the Underground Research Laboratory, Pinawa, Manitoba, Canada [*Martino and Read*, 1994];
7) Two canister-scale heater tests and a heated block test performed within the Basalt Waste Isolation Project, Washington, USA [*Gregory and Kim*, 1981];

8) Heated room experiments [*Metalucci et al*., 1982; *Munson et al*., 1988; 1989] in a salt formation within the Waste Isolation Pilot Plant (WIPP) Project in New Mexico, USA

In the United States, Yucca Mountain, Nevada, with its fractured welded tuff, is the site of the proposed national high-level radioactive waste repository. Thermal tests conducted in granite at Climax, Nevada, in the early 1980s included a spent-fuel test involving eleven fuel canisters and six electrical heaters [*Majer and McEvilly*, 1985; *Patrick*, 1986; *Wilder and Yow*, 1987]. Other tests carried out in the G-tunnel of the Nevada Test Site in volcanic tuff included the Heated Block Experiments [*Zimmerman et al*., 1986a], the Small Diameter Experiments [*Zimmerman et al*., 1986b], and a prototype engineered barrier test [*Ramirez et al*., 1991]. In the mid- and late-1990s, with the construction of the Exploratory Studies Facility, an underground testing laboratory at Yucca Mountain located within a tunnel 8 m in diameter and 8 km in length, the Department of Energy Yucca Mountain Project developed a unified thermal testing strategy, initiating three large-scale field tests, all conducted in the welded, fractured rock that will host the repository. The three tests are the Single Heater Test [*Tsang and Birkholzer*, 1999; *Tsang et al*., 1999]; the Drift Scale Test [*Birkholzer and Tsang,* 2000; *Mukhopadhyay and Tsang*, 2003]; and the Large Block Test [*Lin et al*., 2001; *Mukhopadhyay and Tsang*, 2002].

The proposed repository at Yucca Mountain is unique among its counterparts around the world in two aspects. First, the repository horizon is situated several hundreds of meters above the water table. Therefore, the repository rock (of densely fractured welded volcanic tuff) is partially saturated with water, and thus flow and transport there would involve both liquid (water) and gas (air) phases, even at ambient temperatures. Second, the United States repository design will be such that the radioactive decay heat from the spent fuel would give rise to temperatures in the repository above the boiling point of water for hundreds of years, during which period a phase change between liquid water and vapor would take place within the rock.

In the early 1980s, to acquire an understanding of the processes important for determining the safe performance of a geological repository, scientists working on the Yucca Mountain Project initiated modeling of thermally driven hydrological processes in partially saturated fractured rock. They achieved a progressively improved understanding of such processes over subsequent years. Particularly significant advances were made since the beginning of the field thermal-test program at the Yucca Mountain Exploratory Studies Facility in 1996. Measurements planned for the three *in situ* thermal tests were determined based on the anticipated coupled thermal, hydrological, chemical, and mechanical processes. The large set of data generated from the field thermal tests provided the unique opportunity for testing of coupled-process models. Modeling that is not the subject of this review paper—incorporating coupled chemical [*Xu et al.*, 2001; *Spycher et al.*, 2003; *Sonnenthal et al.*, 2005; *Mukhopadhyay et al.*, 2006] and mechanical [*Rutqvist et al.*, 2004; 2005] processes—was initiated in the late 1990, and progressed in earnest with the carrying out of the eight-year-long Drift Scale Test.

This paper focuses on the modeling of thermal-hydrological (TH) processes in a partially saturated fractured rock formation. Whereas the studies that will be discussed in this paper were almost exclusively motivated by specific concerns over flow and transport around a potential radioactive waste geological repository at Yucca Mountain, the approach and results of these studies are in fact critical in gaining a *fundamental, general* understanding of the multiple coupled processes affecting flow and transport in fractured rock. In this way, these studies are also of interest to the geosciences research community at large, because they address issues relating to geothermal energy, enhanced oil recovery, environmental restoration of hydrocarbon contaminated sites, and geological sequestration of CO_2 to combat global climate change.

PROBLEM DEFINITION

A fractured geological system is characterized by an orders-of-magnitude difference between the permeability of fractures and the rock matrix. For example, the welded tuff of the repository rock at Yucca Mountain has very low permeability, on the order of 10^{-18} m^2 [*Flint*, 1998, *Ghezzehei and Liu*, 2004]. Under ambient conditions, the very small pores of the matrix welded tuff are about 90% filled with water [*Tsang et al.*, 1999, Section 2.5], held in place by strong capillary suction. The welded tuff at the proposed repository horizon is also intensely fractured, with fracture frequency, for fractures with length exceeding one meter, on the order of 3 to 4 m^{-1}. This kind of fracture frequency, with average fracture lengths larger than the average fracture spacing, implies that the fractures are well connected, and that the fractures as a whole act like a continuum as far as fluid flow is concerned. At ambient conditions, these fractures are mostly drained of water because of their weak capillarity (compared to that of the rock matrix) and are therefore the preferred conduits for air flow. The parameters for multiphase flow in a partially saturated formation are represented by characteristic curves [*Scheidegger*, 1974]—that is, (1) the relative permeability to liquid (and gas) as a function of liquid saturation (the smaller the liquid saturation, the lower the liquid phase relative permeability) and (2) the capillary pressure as a function of liquid saturation (the smaller the liquid saturation, the stronger the negative capillary pressure).

In the proposed repository at Yucca Mountain, the heat generated from the decay of radioactive waste is expected to raise the temperature of the water in the rock matrix pores, and as the formation temperature reaches boiling, vigorous vaporization occurs. The pressure increase associated with vaporization gives rise to forced convection of the gas phase, driving the vapor away from the heat source. Because the low capillarity in the fractures favors gas-phase rather than the liquid-phase flow, the vapor thus generated most likely moves into the fractures. As the vapor moves away from the heat source and encounters cooler rock, it condenses, releasing latent heat and slightly increasing the local liquid saturation (very slightly, since the amount of condensate is small) in the fractures. Part of the condensate may then be imbibed into the matrix, where it is subject to a very strong capillary gradient back toward the drier rock, giving rise to a reflux of liquid back to the heat source. Because the capillary suction in the fractures is weak, liquid flow in the fractures is not likely controlled by capillary forces, but rather by downward drainage owing to gravity. A schematic of the coupled TH processes within partially saturated fractured rock near the radioactive-decay heat source is shown in Figure 1. Figure 1 implies that the heat source is in a drift. Since the drift also has high permeability and zero capillary pressure, similar to a rock fracture, it also acts as a conduit for flow of vapor generated in the rock matrix when the pore water boils.

Phase-transformation and the fluid-flow effects described above give rise to a spatial redistribution of moisture in the rock mass. These effects are also reflected in the temperature readings, which would first rise until boiling and then would remain at boiling as long as not all the water in the rock at the temperature-sensor location has vaporized. The plateau in temperature (versus time and space) at a nominal boiling point where two-phase conditions prevail is indicative of substantial heat fluxes being transmitted (because of phase changes) over regions with a small temperature gradient, and is usually referred to as a heat-pipe [*Eastman*, 1968] temperature signature. The processes here in fractured rock differ from a mechanical heat pipe, where the counter flow of liquid and vapor is equal in magnitude so that water is not depleted. Here, in a fractured formation, the return liquid flow from the cooler rock is predominantly via the rock matrix, with orders of magnitude lower permeability than that of the fractures for vapor flow. Hence, water at the location of the sensor (which had registered a temperature plateau) will eventually be boiled away, and temperature will rise above boiling. Based on the above, measurements to monitor TH processes would involve pressure, temperature, spatial distribution, and time evolution of the water content, commonly expressed as liquid saturation, in the rock matrix and fractures.

Table 1 lists the individual thermal-hydrological processes that operate in concert to produce the physical phenomena illustrated in Figure 1. Because the physical phenomena are a product of the different processes that are coupled, it is not possible to obtain a one-to-one correspondence between one single process and one single measurable quantity. For this reason, numerical modeling is one of the key tools in studying coupled processes, and the development of numerical tools that incorporate all the processes listed in Table 1, and their interactions, is also essential to coupled processes research.

EVOLUTION OF CONCEPTUAL MODELS

Historically, the capability for modeling strongly heat-driven multiphase flow in a hypothetical nuclear waste repository is borrowed from techniques used in simulating geothermal reservoirs and enhanced-oil-recovery operation, as discussed in a review article by *Pruess and Wang* [1987]. In the 1980s, several numerical simulators for nonisothermal flow in variably saturated media became available [*Pruess and Wang*, 1984; *Bixler*, 1985; *Travis et al*., 1985; *Polluck*, 1986; *Pruess*, 1987]. These all employ generally similar mathematical and numerical methods and incorporate a large number of complex TH processes such as those listed in Table 1. The study by *Pruess* et al. [1985] using the TOUGH numerical code was an early attempt to incorporate most of the processes shown in Table 1 for a quantitative description of fluid and heat flow near high-level waste containers emplaced in partially saturated fractured rock. A mathematical formulation for the TH processes, within the framework of mass and energy conservation, is presented in Appendix A.

Appendix A shows that in the formulation for fluid flow, Darcy flow is applied to the gas and liquid phases separately, with characteristic curves (relative permeability and capillary pressure) [e.g., *van Genuchten*, 1980] employed to describe the interference between the phases. In the gas phase, binary diffusion between air and water vapor is also included. Heat transport occurs by conduction and convection from TH coupling, including the transport of latent heat associated with phase changes.

Spatial discretization in the numerical models is generally carried out by a finite element (e.g., *Travis et al.*, 1985, *Bixler*, 1985) or finite difference scheme [*Polluck,* 1986]. *Edwards* [1972], *Narasimhan and Witherspoon* [1976] developed an integral finite-difference method that allows great flexibility in grid geometry compared to typical finite difference spatial discretization schemes. Gridblocks, also referred to in the literature as elements, can be of arbitrary shape and size, and can be connected to as many or as few neighboring gridblocks as desired. The entire geometric information of the space discretization is provided in the form of a list of gridblock volumes, interface areas for connections, distances between gridblocks, and components of gravitational forces along connections. Therefore, there need be no reference to a global system of coordinates, or to the dimensionality of a particular flow problem. Heterogeneity of a geological system is accounted for by assignment of different rock properties to respective gridblocks.

The integral finite difference scheme is adopted in the numerical code TOUGH [*Pruess*, 1987], which also offers a number of equation-of state-modules for different fluids to customize the code to the problem at hand. For the thermally driven hydrological system, all water properties are represented by steam table equations. Air is approximated as an ideal gas, and additivity is assumed for air and vapor partial pressures in the gas phase. The solubility of air in liquid water is represented by Henry's law. The equation of state module utilizes the gas-phase pressure, gas-phase saturation, air mass fraction/air partial pressures, and temperature as the primary variables. Mathematical formulation in terms of these variables for the TH processes is presented in Appendix A.

Prior to the mid 1980s, the model simulations of thermal effects within a high-level nuclear waste repository either included no fluid flow and modeled heat transfer by conduction only [e.g., *St. John*, 1985], or made no allowance for vaporization or vapor transport [e.g., *Mondy et al.*, 1983]. By the late 1980s, the TH processes listed in Table 1, and their interactions as described above, are generally incorporated into simulation codes [e.g., *Nitao*, 1993; 1995] and associated numerical studies.

Representation of Fractures and the Effective-Continuum Approximation

Apart from the complexity of multiple processes, modeling of the TH conditions following emplacement of radioactive waste at the proposed repository at Yucca Mountain is further complicated by the presence of fractures in the welded tuff. While the rock matrix can be represented as a homogeneous porous medium, the conceptualization of the discontinuous fractures is a different matter. *Pruess et al.* [1990a] presented numerical simulations of fluid flow, heat transfer, and phase transformation processes induced by decay heat in the fractured welded tuff. The study probed how the geometrical discontinuities—the fractures—affect the TH processes. *Pruess et al.* [1990a] solved the problem in two dimensions in which gravity is neglected. The fractures were represented explicitly as an idealized system of equally spaced horizontal parallel-plate fractures intersecting an infinite string of waste containers (heat source) emplaced in a drift, as shown schematically in Figure 2., Formation parameters, such as fracture and matrix porosities, and their respective permeabilities were chosen as representative of the partially saturated fractured tuff at Yucca Mountain [*Pruess et al.* 1990a]. The highly idealized geometry allowed representation of individual fractures, and the model results afforded insight into detailed TH behavior on the scale of individual fractures and matrix blocks. The results from *Pruess et al.* [1990a] clearly demonstrate the key role of fractures as conduits for vapor flow, while liquid flow mainly takes place in the rock matrix, as pore water boils in response to a strong heat source.

Although the above approach of representing fractures explicitly in the numerical discretization scheme is conceptually straightforward and well suited for fundamental studies of an idealized system, it is not practical for most "real" problems. For a real fractured rock mass, the amount of geometric detail that needs to be included would be far beyond the capacity of current digital computers. Even if computationally feasible, a detailed, explicit treatment of all fractures is not desirable in practice, since there are seldom, if ever, adequately detailed measurements to provide a realistic representation of the fracture geometry. Moreover, in modeling TH conditions, one is usually interested in predicting averages over some macroscopic measurement scale, and so much detail on the level of individual fractures would inevitably be redundant.

Based on the TH behavior observed in the simulations in *Pruess et al.* [1990a], which explicitly consider effects from individual fractures, *Pruess et al.* [1990b] presented an effective continuum model to describe fluid and heat flow in fractured porous media that mimics the explicit fracture and matrix simulation results. The crucial concept underlying an effective continuum approximation is the assumption of a local thermodynamic equilibrium between rock matrix and fractures. In this simplified approximation, fluid and heat flow in a fractured porous medium is represented by means of a single effective or "equivalent" continuum. The equivalent continuum is defined as one that will yield the same mass fluxes, temperature, pressure, and saturation distributions as an explicit discrete fractured-porous matrix model, given the same initial and boundary conditions for the two models. Implicit in this definition is that the many fractures can be approximated as a continuum, characterized by (continuum) fracture parameters, in the same manner as the rock matrix is represented by a porous continuum characterized by the matrix parameters.

Instead of requiring two sets of characteristic curves, one for the fractures and the other for the matrix, one set of effective-continuum-model characteristic curves (relative permeability and capillary pressures as a function of saturation) was developed in terms of fracture- and matrix- continuum properties [see also *Peters and Klavetter*, 1988]. Where applicable, this approximation provides substantial simplification and computational economy, and the effective continuum approximation can closely match predictions obtained from an explicit modeling of fracture effects. The criterion for the maintenance of local thermodynamic equilibrium between the matrix and fractures is that during the time required for the diffusive processes perpendicular to the fracture plane to penetrate to the mid-plane between two fractures (c.f. Figure .2), the radius of the propagation of the perturbation is “small” [*Pruess et al.*1990b]. Hence, the effective continuum approximation breaks down for processes involving rapid transient perturbation or extremely low-permeability rock matrix and large fracture spacing. Note that, based on the criterion given above, regardless of the applicable thermal and hydrological parameters, approximation will be valid at “sufficiently” large times or distances. *Pruess et al.* [1990b] show that for Yucca Mountain repository rock, the effective continuum approximation is valid for time much longer than 0.89 days, and distance much larger than 0.5 m. Furthermore, if the fracture spacing were so large, then even the approximation of the fractures being represented by a continuum with one set of properties breaks down.

Buscheck and Nitao [1991] also applied the effective continuum concept to model a field test [*Ramirez et al.*, 1991] involving a heater horizontally emplaced within a borehole in the G-Tunnel complex of the Nevada Test Site. Two alternative models in two dimensions were invoked. One model assumes an infinitely long horizontal heater, orthogonally intersected by uniformly spaced fractures—a configuration similar to that of Figure 2. The other model volume averages the matrix and fracture properties through the use of effective continuum approximation. Heat flow was found to be dominated by conduction, and the effective continuum model was found to adequately represent drying behavior within the rock.

Effect of Fractures and the Dual-Permeability Model

When equilibration between matrix and fractures is “slow” compared to the external perturbation (in other words, when local thermodynamic equilibrium between fractures and matrix cannot be assumed), then fractures and matrix must be modeled separately. An early approach to modeling flow in fractured media is the double-porosity method, originally developed by Russian hydrologists [*Barenblatt et al.*, 1960] and introduced into the petroleum literature by *Warren and Root* [1963]. Here, a fractured porous medium is partitioned into a primary porosity, composed of small pores in the rock matrix, and a secondary porosity, composed of a well-connected network of fractures. Each of the two porosities is treated as a continuum whose properties can be characterized by customary porous-medium properties, such as permeability, porosity, and compressibility. Note that the very fact that fractures may be treated as a continuum implies that the fracture density must be such that the fractures are “connected,” or that the spacing of fractures should be small relative to the fracture lengths. Flow within each continuum is assumed to be governed by Darcy's law—that is, driven by pressure gradients.

In the classical double-porosity model, global flow in the medium occurs only through the fracture continuum, while the rock matrix interacts locally with the fractures by means of "interporosity" flow, for which a quasi-steady approximation is made. However, the assumption that global flow occurs only through the network of well-connected fractures breaks down for multiphase systems with strong capillary effects, such as that in the partially saturated rock at Yucca Mountain [*Doughty*, 1999]. Here, the wetting phase(s) (e.g., water) will preferentially occupy the small pores in the rock matrix, while the nonwetting phase(s) (e.g., air and vapor) will tend to reside in the largest voids—the fractures. In this situation, advective flow (permeability) must be permitted in both the fracture and matrix continuum. Flow systems with two kinds of permeability have sometimes been referred to as "dual-permeability" [*Miller and Allman*, 1986], as distinct from "double-porosity" reservoirs. Dual-permeability reservoirs are encountered in partially saturated groundwater systems, in geothermal reservoirs, and in oil and gas fields. Because the dual-permeability approach is more computationally demanding than the effective continuum model approximation, in that the number of discretized gridblocks for the former is double that of the latter, the dual-permeability approach only became commonly implemented in the late 1990s, when ever-faster and ever-larger-memory computers became available. Currently, the dual-permeability approach is the Yucca Mountain Project norm for most modeling pertaining to the fractured repository rock [e.g., *Wu et al.*, .1999; 2002].

Computational Constraints and Advances

Computational feasibility not only constrained earlier modeling work at Yucca Mountain to the effective continuum approach (where fractures and matrix are treated together as one single continuum); it also limited such work to two dimensions, using rather coarse grids. By the mid-1990s, advances in computational capability made it possible for numerical models composed of tens and hundreds of thousands of gridblocks to be routinely applied to coupled-processes problems modeled in three dimensions. It also became possible to incorporate realistic geological features (including heterogeneity effects) and geometries in the numerical models. These advances, together with the increasing accessibility of parallel computing, greatly improved the utility of numerical modeling in simulating complex, thermally induced processes. They also enabled application of coupled-processes modeling to address the key repository performance issues with increased levels of confidence.

Gas-Phase Flow and Enhanced Vapor Diffusion

Interest in gas-phase flow at Yucca Mountain arose initially from the concern that a few radionuclides, such as ^{14}C, could be transmitted through gaseous pathways [*Von Konynenburg et al.*, 1985, 1986]. Hence, an understanding of gas-phase flow effects was thought necessary for determining the quantity of gaseous radionuclides that could be released at the land surface. This earlier concern was shown to be not a public health issue in the Environmental Impact Statement [*DOE*, 2002, Appendix I Section 7]. Besides providing potential pathways for radionuclides to the accessible environment, gas-phase flow effects may indirectly influence the distribution of moisture and liquid-phase flow through vaporization and condensation processes associated with vapor transport. *Tsang and Pruess* [1989, 1990] performed modeling studies of gas movement and moisture redistribution processes mediated by gas-phase flow and diffusion, under ambient conditions prior to emplacement of radioactive waste. Study results showed that moisture removal from Yucca Mountain (arising from a lowered humidity of the soil gas at the land surface) was controlled by vapor diffusion, while other factors, such as the stratigraphy for alternate layers of welded and nonwelded units, and the choice of characteristic curves, played an insignificant role.

Along the same lines, soil science literature up to the early 1990s indicated considerable experimental evidence of vapor-diffusion enhancement, by two to three orders of magnitude over the textbook binary diffusion formula of a free-space diffusion coefficient multiplied by the porosity, gas phase saturation, and a tortuosity factor. The latter three parameters account for effects of the geological formation on the diffusion process. There was a hypothesis attributing the enhancement of vapor diffusion to phase changes occurring on opposite ends of the water-filled small pores. The phase changes would overcome the obstacle posed by the small pores to the flow of condensable gas, vapor. The phase-change mechanism would not be applicable to the noncondensable gas, air. However, no quantitative theory based on this hypothesis existed in the literature, and hence enhanced vapor diffusion remained mainly an experimental observation. Therefore, *Tsang and Pruess* [1990] performed a sensitivity study by varying the vapor-diffusion parameter by several orders of magnitude. Simulation results indicated that the rate of moisture removal from vapor transport had an upper limit of about 0.1 mm/year (for orders-of-magnitude vapor-diffusion enhancement). Such a small moisture removal rate implies that the issue of vapor-diffusion enhancement is incidental to the moisture conditions at Yucca Mountain, and in the absence of actual data, incorporating this effect into coupled-processes modeling is likely unnecessary.

Large-Scale Gas Convection

Following the emplacement of waste in a repository, the heat generated by the waste would provide a driving force for large-scale fluid movement because of the lower density of a heated fluid. Questions naturally arise as to the potential for transport of radionuclides (either in the gas phase or liquid phase) by this kind of buoyancy flow. With this in mind, *Tsang and Pruess* [1987] presented simple estimates for velocities of buoyancy-driven flow of liquid and gas phases around a hypothetical high-level nuclear waste repository in partially saturated, fractured tuff. These estimates indicate that gas-phase convection could take place at a velocity on the order of 20 mm/year, whereas liquid convection is expected to be several orders of magnitude lower, mainly because of the contrast in fracture and matrix permeability. In the same paper, *Tsang and Pruess* (1987) presented a numerical simulation on the mountain scale in two dimensions, assuming a smeared heat source for the repository, and using an effective continuum approximation. Simulated results confirmed the simple estimates of large-scale fluid flow surrounding the proposed repository. The simulations showed that the dominant mechanism driving the large-scale gas movement was the density change from heating, and that the convection-gas flow pattern persisted for thousands of years after waste emplacement (though the magnitude of this flow peaked at about 100 years).

Effects of Faults on Multiphase Flow

Several large-scale fault zones exist within Yucca Mountain. The effect of such high-permeability, large-scale discontinuities on flow and transport is a question of concern in assessing the site's ability to isolate radionuclides from the biosphere. *Tsang et al.* [1993] presented a numerical study investigating how faults affected both liquid- and gas- phase flows in the natural state of Yucca Mountain prior to waste emplacement, (as well as after waste emplacement when the fluid flow is strongly heat-driven). This numerical study was partly motivated by the lack of direct measurements for fault properties. Faults were conceptualized to be a "broken-up" version of the original formation, and the finely broken-up material within the fault was hypothesized to give rise to a saturated permeability considerably larger than that of the "unbroken" formation.

Two alternative representations were considered. One had large pieces of original formation interspersed among more finely broken-up material (i.e., a "double-porosity" representation); the other had the entire fault filled with finely broken-up material (i.e., a "single-porosity" representation). The finely broken-up material was given a large saturated permeability, 4.4×10^{-11} m^2, typical of fractures in the Yucca Mountain welded tuff, and a relationship between saturated permeability k_s and capillary radius r_c ($k_s = r_c^2/8$) (from the measured data of Yucca Mountain tuffs, Apache Leap tuffs, and Las Cruces soil) was imposed on the characteristic curves. Based on simulation results from the conceptualization in *Tsang et al.* [1993], a fault plays little role in channeling water into itself. However, the fault can enhance the upward gas flow after waste emplacement, which has implications for the transport of gaseous radionuclides.

ADVANCES IN MODELING AND THEIR APPLICATION TO *IN SITU* FIELD THERMAL TESTS

By the mid-1990s, numerical codes that incorporate coupling between the thermal and hydrological processes have become commonly available. Not surprisingly, these numerical tools were developed within the United States Department of Energy Civilian Radioactive Waste Management Program, driven mainly by program need. The simulation codes are respectively NUFT (*Nitao*, 1993; 1995) and TOUGH2 (*Pruess*, 1991; *Wu et al*., 1996).

As mentioned above, at about the same time, beginning in 1996, following the construction of the underground tunnel, the Exploratory Studies Facility, the Yucca Mountain thermal testing program implemented two *in situ* field tests in the repository unit of the middle nonlithophysal Topopah Spring welded tuff (Tptpmn) within the Exploratory Studies Facility: the Single Heater Test and the Drift Scale Test. In addition, a Large Block Test was performed in an outcrop of the Tptpmn in Fran Ridge, a short distance from the north entrance of the underground tunnel. The objective for all three thermal tests was to acquire an in-depth understanding of the coupled processes—thermal, hydrologic, chemical, and mechanical—recognizing that a fundamental understanding of these coupled processes, including the ability to model and predict with confidence their effects over periods of time unprecedented in engineering, is essential for demonstrating the effective isolation of nuclear waste through geological disposal. The three tests complement each other. The Single Heater Test served as a pilot run pertaining to measurement systems, testing strategy and modeling methodologies to be implemented in the much larger-scale and longer-duration Drift Scale Test. Instrumented to measure thermal, hydrological, chemical, and mechanical coupled processes, the Single Heater Test had an emphasis on the mechanical aspect of the coupled processes. The Drift Scale Test's design was intended to closely pattern after that of the repository at Yucca Mountain. (The repository design at the time of the Drift Scale Test had an interdrift spacing of 30 m, as opposed to that of 81 m for the current design). The Large Block Test, because it was conducted in an outcrop, afforded better controlled boundary conditions than those of the Single Heater Test and the Drift Scale Test, carried out underground. It also had the additional objective of evaluating newly developed measuring systems, including that of measurement of *in situ* thermal conductivity and thermal diffusivity through the use of a Rapid Estimation of K and Alpha (REKA) probe [*Danko and Mousset-Jones*. 1991; *Danko et al.*, 1998].

The approach to meeting the test objective (to better understanding of coupled processes) was a close integration of sophisticated and detailed numerical modeling with measurements. Such an approach is feasible partly because of the great advances in computing capability, thus enabling test predictions to be carried out with numerical models faithful to the realistic test geometry in three dimensions, with sufficiently fine discretization and without the need to resort to simplifying assumptions with regard to TH processes (such as those listed in Table 1 and illustrated schematically in Figure 1) because of computation constraints.

Figure 1 indicates that one of the main manifestations of the coupling of thermal and hydrological processes listed in Table 1(heat conduction, heat convection, liquid and gas flow in the rock matrix and the fractures, vaporization, and condensation) is the redistribution of moisture in the rock mass. That is, drying will occur near the heat source, with a corresponding condensation zone beyond the drying; and over time, these drier and wetter zones will migrate out, away from the heat source. In addition, the presence of water and the associated phase change to vapor results in a distinctive temperature signature at the boiling point of water. This temperature signature from TH coupling, though distinctive, is subtle, because most temperature increases in the rock mass derive from heat conduction, the dominant heat-transfer process. Because the multiple processes listed in Table 1 operate in concert to produce the observable phenomena of moisture redistribution and temperature signature, there is not a one-to-one correspondence of an individual process listed in Table 1 to a particular measurable parameter. This inherent inability to correlate one process to one measureable quantity necessitates reliance on numerical modeling in the study of coupled processes. The rationale is that only when the numerical model had incorporated all the relevant multiple processes would it be able to reproduce the observed phenomena. Therefore, good agreement between the modeled and measured moisture redistribution, and the TH signature in the temperature data, is interpreted to mean that the TH processes operating in the geological system are indeed those incorporated in the numerical model, and that we have gained an understanding of how these processes are coupled.

Results from this close integration of modeling and testing have been extremely encouraging. The agreement between model predictions and test measurements reinforces what was learned in the early modeling studies discussed in the previous section, and the detailed examination of the data and predictions refines our fundamental understanding of the coupled TH processes at such a site. In the following, we shall briefly summarize and present examples from the three field tests to illustrate how the close integration of modeling and measurements enables us to track the complex processes we seek to understand. The examples presented below employ the numerical simulator TOUGH2 [*Pruess*, 1991; *Wu et al.*, 1996; *Pruess et al.*, 1999], a higher generation of the code TOUGH [*Pruess*, 1987] discussed earlier. TOUGH2 is widely used in the international research community for addressing problems such as environmental restoration, geothermal and petroleum reservoir engineering, carbon sequestration, and nuclear waste isolation. The breadth of the utility of this numerical tool for studying coupled processes can be seen from the programs and proceedings of periodically held international TOUGH2 workshops (in 1995, http://www-esd.lbl.gov/TOUGH2/worksh95/T95.doc.html; in 1998, http://www-esd.lbl.gov/worksh98; in 2003, http://wwwesd.lbl.gov/TOUGHsymposium03/index.html; and in 2006, http://www-esd.lbl.gov/TOUGHSymposium) .

Single Heater Test

The Single Heater Test consisted of a 5 m long heating element, at a nominal 4 kW, emplaced horizontally among 30 instrumental boreholes spanning a rock block approximately 13 m × 10 m × 13 m (Figure 3). The Single Heater Test had a heating period of 9 months, starting in August 1996. Temperature in the rock rose to boiling within a few days of heat initiation in a sensor located at 0.3 m from the center of the heater hole. The highest temperature recorded in the same sensor at the end of the heating period was 165^{o}C. Thermal and hydrological properties important for input to the coupled-processes modeling were obtained from extensive preheating characterization of the Single Heater Test block. These site-specific data [*Tsang et al.*, 1999] included laboratory measurements of grain density, matrix porosity, and liquid saturation, thermal conductivity at different liquid saturation, heat capacity, and thermal expansion coefficients. Since fractures play a key role in TH processes, fracture permeability was obtained from preheating characterization by air-injection tests within the 30 boreholes in the test block [*Tsang et al.*, 1999; *Huang et al.*, 1999]. Steady-state pressure responses in the injection borehole were used to calculate the local fracture permeability around each injected zone. The interference pressure response in all boreholes other than the injection borehole indicated that the fractures in the Single Heater Test block were well connected, and that the gas flow in the fractures resembled more that of flow through a heterogeneous continuum. Hence, the measured local fracture permeability derived from the pressure response in each injection borehole was that of the fracture continuum, and the range of values obtained from testing in different boreholes represent the statistical distribution of the heterogeneous fracture continuum permeability field.

Modeling of the Single Heater Test [*Birkholzer and Tsang*, 1997; *Tsang and Birkholzer*, 1999] was carried out in three dimensions. The 3-D grid representation of the test block has about 30,000 gridblocks, with more than 100,000 connections among them. Fine gridding and radial symmetry was maintained around the heater hole to be compatible with sharp gradients of temperature, saturation, and pressure. The fractured welded tuff in which this test took place was conceptualized as a dual continuum. Laboratory measurements of rock-core hydrological properties were assigned to the matrix continuum, whereas assignment of fracture permeability values was based on site-specific field air-injection measurements. As stated above, the local permeability determined from air injection in the 30 borehole take on a range of values, reflecting the heterogeneous nature of the fracture continuum. Only one “average” value to the entire test block, the median of all values, 5.8×10^{-14} m^2, was chosen to represent the background fracture continuum permeability. A geometric mean is commonly used to characterize a stochastic heterogeneous field in the literature. The median value of the measured values from the 30 boreholes in the Single Heater Test block is very similar to the geometric mean of all the measured values.

Since the combined data of fracture mapping, borehole video logs, and air-injection interference tests indicated the presence of a high-permeability discrete feature, about 4 m in extent, the numerical model also included a high permeability zone to the southwest of the heater, superposed on the uniform background permeability. This high-permeability discrete feature was given a permeability value of 5.2×10^{-12} m^2, the local measured value. (Readers are referred to *Tsang and Birkholzer* [1999] for a detailed discussion of the numerical model and input parameters.). This numerical model—portraying the realistic 3-D test geometry and incorporating all relevant TH processes (listed in Table 1)—was used to make predictions of the test outcome prior to the test. Test results were then evaluated against simulation predictions as the test progressed.

Coupled TH processes were anticipated to manifest themselves in (1) a heat-pipe signature within the temperature profiles and time history, and (2) the evolution and spatial distribution of the test block drying and condensation zones. For observation of the former, numerous temperature sensors were installed in boreholes within the test block; for the latter, neutron logging, crosshole radar tomography, and electrical resistivity tomography were carried out at periodic intervals to probe moisture-content changes in the rock-matrix pores. Further, since gas flow occurs predominantly in fractures (liquid saturation in the fractures at ambient conditions is expected to be less than a few percent), periodic air-permeability measurements throughout the test in selected boreholes targeted the time evolution of liquid saturation changes (wetting) in the fractures. An increase in the liquid saturation means reduction of fracture pore space available for air flow, which translates into a reduction of fracture permeability to air. The observed data agree well with the model predictions [*Tsang and Birkholzer*, 1999]. In the following, we present some selected results.

Figure 4 shows the simulated predictions of the temperature as a function of radial distance from the heater in the mid-heater plane, compared to that recorded by the temperature sensors, at 9 months of heating. Also included in the figure are results from a numerical sensitivity study, in which fluid flow was excluded from the numerical model, so that heat transfer in the rock resulted from thermal conduction alone. Thermal-conduction-alone results shown in Figure 4 correspond to two thermal conductivity values: that of the laboratory-measured “dry,” 1.67 W/(m K), and “wet,” 2.0 W /(m K). (Eq. A12 in Appendix A gives the functional dependence of thermal conductivity on liquid saturation). Graphs in Figure 4 demonstrate that heat transfer in the Single Heater Test was dominated by heat conduction. However, TH effects on temperature, though small in magnitude, are significant for a good match to the observed data. Because there were no temperature sensors at the exact location of the plateau at the boiling temperature shown by the simulation, the presence of that plateau, due to TH coupling, can only be inferred from the general slope and shape of the measured temperature data, and how they differ from the heat-conduction-only simulations. Note also that the simulated temperature for the matrix and fracture continua is almost identical.

Figures 5 and 6 illustrate the fracture liquid saturation changes from wetting and drying, tracked by air-permeability measurements and matched by model simulations. Figure 5 shows the simulated fracture-liquid-saturation contours, from a full 3-D numerical model of the Single Heater Test, after three and nine months of heating and after three months of cooling, in the vertical plane of boreholes 16 and 18, orthogonal to the heater. These boreholes, one above the heater plane and the other below the heater plane, were installed with high-temperature inflatable packers separating the borehole into three zones, air-injection lines, and pressure sensors for air-permeability measurements. Zone 3, as indicated in Figures 5 and 6, reaches to the end of each borehole. The liquid-saturation contours in Figure 5a show that at three months after heating started, drying occurs around the heater; while wetting from vapor condensation occurs beyond the drying zone farther from the heater. The contours also display significant gravity drainage in the fractures. The liquid saturation contours in Figure 5b at nine months of heating, end of heating phase, are qualitatively similar to that at three months of heating. Quantitatively, the drying zone is larger, the drainage less, at nine months than at three months of heating. On the other hand, contours at three months of cooling in Figure 5c show that whatever saturation that has built up in the fractures as a result of condensation has disappeared, because of gravity drainage and matrix imbibition. This is because during cooling, the condensed water drained away or imbibed into the matrix is no longer replenished by condensation of a constant supply of vapor, produced during the heating phase from boiling of the pore water in the matrix.

The air-permeability measurements shown in Figure 6 are consistent with the predictions of the 3-D numerical model for the Single Heater Test in Figure 5. Specifically, in Zone 3 of boreholes 16 and 18, where modeling results predict an increase in liquid saturation, resistance to airflow increases and air-permeability values decrease. (The horizontal axis of Figure 6 is the time line with the heater activation and termination dates marked; the vertical axis is the air permeability.) Graphs in Figure 6 show a decrease in air permeability (from the preheated values) by a factor of four and two, respectively, for Zone 3 of boreholes 16 and 18, during the entire heating phase of the Single Heater Test. The air permeability returns to slightly above preheat values[1] after the termination of heating. For Zones 1 and 2, the air-permeability values remain at their preheat values (not shown here) throughout the test, attesting to no change in resistance to airflow. These measurements are consistent with the predicted fracture liquid saturation contours from the TH model (Figure 5), which show little increase in liquid saturation in Zones 1 and 2 during the heating phase.

Temperature and liquid saturation (*Buscheck*, 1998; Hardin, 1998 Chapter 3) for the Single Heater Test simulated using the numerical code NUFT (*Nitao*, 1995; 1998), developed at the Lawrence Livermore National Laboratory are similar to those in Figures 4 and 5.

Drift Scale Test

Figure 7 shows a 3-D perspective of the Drift Scale Test, which involved a multitude of heaters (color coded red) and close to 100 instrumented boreholes for measuring thermal, hydrological, mechanical, and chemical processes. Activation of heat commenced on December 3, 1997, and continued for a little over four years, until

---

[1] Temperature in Zone 3 is higher postheat than preheat, implying some net drying.

January 14 of 2002. Measurements in the test block continued following the turning off of heat, for four years of natural cooling. The heat power during heating phase is about 180 kW. The Drift Scale Test centers around the Heated Drift, having a 47.5 m long heated section separated from the unheated section by a thermally insulated bulkhead. Heating is provided by nine canister heaters within the Heated Drift, as well as 50 rod heaters, referred to as “wing heaters”, placed in 11.5 m long horizontal boreholes that flank the Heated Drift. The diameter of the Heated Drift is 5 m, similar to the dimension of the current design of the repository emplacements drifts that would contain the radioactive waste containers. The two arrays of wing heaters were included to quickly (in a few months) bring TH conditions in the rock up to those anticipated in the proposed repository only after decades of heating from the radioactive decay of the 70,000 metric tons of waste expected to be disposed at Yucca Mountain.

In addition to being patterned after the proposed repository thermal design, the Drift Scale Test benefited greatly from the insights gained from the previous Single Heater Test. Lessons learned were applied to the Drift Scale Test with respect to the overall testing and modeling approach; to spacing, configuration of boreholes; to instrumentation, and frequency of measurements. A numerical model predicting the performance of the Drift Scale Test was developed [*Birkholzer and Tsang*, 1997] prior to activation of the heaters. Test geometry and dimensions, including the drifts, alcoves, and the decline of the observation drift, were represented realistically in the 3-D numerical model. Comparing the results of the Drift Scale Test simulations [*Birkholzer and Tsang*, 2000] to the rich set of high-quality Drift Scale Test data indicates that the anticipated TH phenomena in the repository fractured welded tuff are indeed being observed, A few selected examples will be cited in the following.

In the Drift Scale Test, simulations were being compared to temperature measurements taken by~1,700 temperature sensors installed in 26 boreholes, grouped in five radial arrays emanating from the heated drift (see Figure 7a and b). Modeled results and measurements are compared in Figures 8 and 9, which show snapshots of the temperature profiles along the eight boreholes (158–165) at 3 months and 18 months of heating, respectively. At 3 months of heating (Figure 8), the temperature is at nominal boiling (~97°C at the elevation of the Drift Scale Test in the mountain) in boreholes 160 and 164, between 1 and 11 m from the borehole collar—these are the two horizontal boreholes parallel to and slightly above the wing heaters. The boiling temperature indicates the presence of both liquid and vapor phases resulting from vaporization and condensation processes induced by close proximity to the wing heaters.

After 18 months of heating (Figure 9), the temperatures in these sections in boreholes 160 and 164, between 1 and 11 m from the borehole collar, significantly exceed 100°C. These temperatures indicate that all the liquid water in the borehole vicinity has boiled away, and that the two-phase zone within the Drift Scale Test block has expanded beyond the locations of the temperature sensors in these sections. However, a small heat-pipe signature at ~12–14 m from the borehole collar appears in these two boreholes, 160 and 164, indicating that at the locations just beyond the tip of the wing heaters, a two-phase zone of vapor and liquid water (denoted by the curve plateau) persists. That the temperature at just beyond the tip of the wing heaters can remain at boiling with ongoing vaporization implies that condensed water is being supplied to the wing heater horizon via gravity drainage from above. Moreover, the heat-pipe signature at ~ 97^{o}C seen in boreholes 161, 163, and 165, at ~2–4 m from the borehole collar, is attributed to the condensation front immediately outside the dry region surrounding the heated drift and the wing heaters. *Birkholzer* (2006a, 2006b) used the heat-pipe signatures in the observed temperature profiles to derive estimates for the magnitude of liquid drainage originating from the condensation front.

These signatures of TH coupling and temperature data (plateaus at ~97^{o}C) are well reproduced in the simulations (*Birkholzer and Tsang*, 2000). A level of qualitative agreement between data and simulations similar to that shown in Figures 8 and 9 is also obtained from the other four radial arrays of temperature boreholes, at different stages of testing, through four years of heating and four years of cooling. Specifically, the data and simulation results show that as heating phase continues, the heat-pipe signatures for boreholes 161, 163, and 165 persist, but their locations increase in distance from the borehole collar, indicating the moving out of the condensation front with heating. Similarly, the temperature plateau in boreholes 160 and 164 located beyond the tip of the wing heater persists throughout the heating phase. Aside from comparing temperature measurements with simulations in terms of snapshots at three-month time intervals, the temperature history for any of the temperature sensors can be compared to simulated predictions. For example, in Figure 10, we show temperature (measured and modeled) as a function of time for six (out of 67) temperature sensors in borehole 160. The match between model prediction and measurements is good. Since it is not feasible in a few figures to display the enormous volume of data collected, we have computed the mean error and the root mean square error (which give an objective and quantitative measure of goodness of fit between simulation and data), utilizing the simulated and measure temperature values for ~1,700 sensors at three-month intervals during the heating and cooling phases. Our computations show that through four years of heating and four years of cooling, the computed root mean error for ~1,700 sensors is less than 5°C.

The time evolution and spatial distribution of moisture changes in the rock matrix from vaporization and condensation are tracked by geophysical measurements such as: neutron logging, crosshole radar tomography, and electric resistivity tomography. We find the model predictions to be consistent with the time and extent of drying and wetting observed in the geophysical data, as illustrated by Figures 11 and 12. Figure 11a, a tomogram of the change in liquid saturation (at the end of the four-year heating phase) constructed from crosshole radar surveys in boreholes 49, 50, and 51 (see Figure 7c for locations of boreholes), displays the drying around the drift and the wing heaters. Figure 11b is the model simulation of change in liquid saturation within the matrix after four years of heating. Figure 12 shows the data from neutron logging in boreholes 47 through 51, as well as the tomogram constructed from electrical resistivity measurements, at about 23 months of heating. The solid line contour represents a simulated matrix saturation of 0.5, showing drying from the ambient preheat matrix saturation of 0.92.

The general agreement between numerical simulation predictions and observations of the key manifestation of the TH processes from the Drift Scale Test provides reassurance that our understanding of the coupled TH processes at Yucca Mountain is sound. This is because the numerical model for the test was constructed prior to the beginning of the test, and there were no adjustments to any parameters afterwards. The model, however, does contain slight modifications/refinements following the beginning of heating— including more faithful representation of the actual test configuration (as-built sensor locations) and test conditions (such as the actual rate of heating versus planned heating rate) than was possible when the model was originally constructed. Also, the first few months of heating-phase data enable us to discriminate between alternative assumptions studied in the preheat predictions [*Birkholzer and Tsang*, 1997]. For example, prior to testing, uncertainty existed as to the effectiveness of radiative heat exchange within the Heated Drift. Modeling of the Drift Scale Test was therefore carried out with two alternative conceptualizations, one completely effective, and the other ineffective, radiative exchange within the drift. The first 60 days of Drift Scale Test data, showing rather uniform drift-wall temperature readings, supported the conceptualization that radiative heat exchange is highly effective in equilibrating the temperature within the heated drift. Thus, this alternate conceptual model of completely effective radiative heat exchange within the drift has been adopted to model the Drift Scale Test [*Birkholzer and Tsang*, 2000].

A TH issue that has raised considerable concern over the course of the Drift Scale Test is that the bulkhead separating the heated side from the unheated side of the Heated Drift is thermally insulated, but not perfectly sealed or impervious to fluid movement. As a result, a substantial fraction of vapor generated within the rock escapes via the highly permeable drift and the bulkhead. The matter of vapor loss through the bulkhead has raised questions as to the validity of, and conclusions drawn from, the TH modeling of the Drift Scale Test. *Mukhopadhyay and Tsang* [2003] specifically address this concern and demonstrate that in the modeling of the Drift Scale Test, the adoption of an open boundary for the bulkhead and the assignment of high permeability values for the wing heater boreholes and the Heated Drift allow vapor to escape from the test block, and that the resultant model predictions (which account for the vapor escape) closely match the experimental data.

Large Block Test

The Large Block Test, having a test block size of 3 × 3 × 4.5 m, was mechanically excavated from an outcrop (of the same repository middle nonlithophysal tuff as the Single Heater Test and Drift Scale Test) in the Fran Ridge area of Yucca Mountain. Heating was provided by electrical heaters in five parallel horizontal boreholes. The spacing of the boreholes, and the heating power of ~450 W for each heater, were such as to result in a planar heat source. The heater holes and some of the other boreholes in the test block are schematically shown in Figure 13. Suites of passive monitoring and active testing measurements, similar to those implemented in the Single Heater Test and Drift Scale Test, were implemented in the Large Block Test. The heating phase extended from February 28, 1997, through March 10, 1998, and natural cooling was monitored until September 1998. As in the Single Heater Test and the Drift Scale Test, the temperature in the rock rose above boiling during heating. The highest temperature measured in the block reached 142°C at about 5 cm below the heater plane. (For a comprehensive description of the design, construction, instrumentation, and data collection systems, the reader is referred to *Lin et al.*, [2001].)

Pretest analysis of the TH response from the Large Block Test can be found in *Wilder et al.* [1998]. The pretest TH analysis was conducted mainly for test design purposes and was in two dimensions, taking advantage of the symmetry afforded by the planar heat source. Following heat initiation, investigators developed a 3-D numerical model for the Large Block Test based on the dual-permeability conceptual model for rock matrix and fractures [*Civilian Radioactive Waste Management System (CRWMS)*, 2000]. The NUFT simulator [*Nitao*, 1995; 1998], which incorporates all the TH processes listed in Table 1, was used. *Lin et al.*, [2001] summarize the comparison of simulation results to the temperature data. As with the Single Heater Test and Drift Scale Test, the model captured in general the dominant effect of heat conduction and the more subtle signature of convection in the data. However, there were some temperature data that were not reproduced by the simulation results. On June 13, 1997, and on September 2, 1997, some sensors that had previously registered temperature above boiling suddenly drop to the boiling point of water. *Lin et al.* [2001] reported that there was evidence that the temperature drop in these sensors on September 2, 1997, was triggered by a rain event, but attributed the temperature drop on June 13, 1997, to a sudden release of overheated water in the rock that flowed down the boreholes.

The data during the rain event on September 2, 1997, presented a unique opportunity to further our understanding of the impact of discrete fracture heterogeneity on thermally driven liquid and gas flow [*Mukhopadhyay and Tsang*, 2002]. In the studies of flow and transport in a fractured rock, heterogeneity is often responsible for discrepancies between data and simulation by models where heterogeneity is not specifically accounted for. The effect of heterogeneity on flow is often more prominent under ambient conditions than under thermal conditions. This is because the manifestation of TH coupled processes from strongly heat-driven flow—boiling, vaporization, and condensation—tend to "mask" the effects of heterogeneity. In other words, the perturbation of flow from heat is stronger than that from small-scale heterogeneity. Indeed, this is the reason that the representation of the densely fractured tuff as a fracture continuum (in modeling of the Single Heater Test and the Drift Scale Test) can reproduce the temperature and moisture redistribution data well. The rain event during the Large Block Test, likely resulting in rapid flow down fractures, apparently gave rise to a situation in which the perturbation caused by heterogeneity overrode the homogenizing effect of heat, thus affording an opportunity to examine the effect of heterogeneity on TH processes.

To explore the effect of discrete-fracture heterogeneity on thermally driven liquid and gas flow, *Mukhopadhyay and Tsang* [2002] constructed a numerical model in three dimensions for the Large Block Test, in a manner similar to that discussed earlier for the Single Heater Test and the Drift Scale Test—employing first the dual-continuum model, in which fractures were represented as a homogeneous continuum. This model was able to capture the general trend of the temperature data, dominated by heat conduction, and tempered with subtle heat-pipe signature. *Mukhopadhyay and Tsang* [2002] then incorporated discrete fracture effects into the numerical model to focus on the data surrounding the abrupt temperature drops on June 13, 2007, and September 2, 2007. Some results from *Mukhopadhyay and Tsang* [2002] are discussed in the following.

A portion of the temperature data collected by sensors in two vertical boreholes TT1 and TT2 (Figure 13) shows a sharp drop and subsequent oscillation at around 4,470 hours (of heating). *Mukhopadhyay and Tsang* [2002] hypothesized that these seemingly anomalous data are associated with a thunderstorm event that occurred on September 2, 1997. Since the Large Block Test was open to the atmosphere, this event must have caused infiltration of rainwater (despite the insulation covering of the test block) down the fractures, and even down to the plane of the heaters. A careful study of the temperature data, recorded by the different sensors both above and below the heater plane along the two boreholes (TT1 and TT2) immediately before and after the rain events, led to the belief that local discrete, permeable features/fractures are responsible for these seemingly anomalous temperature data.

To test the hypothesis with the model, three discrete features (consistent with detailed fracture mapping data of the test block) were incorporated into the otherwise dual-continuum representation of the Large Block Test. Two were vertical features, 0.001 m thick, located in close vicinity to the temperature boreholes TT1 and TT2, and were assigned a permeability two orders of magnitude higher than that of the background fracture continuum value elsewhere in the test block. A third inclined discrete feature, with an angle of 75^o from the horizontal axis, given a permeability value two orders of magnitude higher than even that of the two vertical discrete features, was added to intersect the vertical feature near TT1. By invoking the local heterogeneity comprised of these three discrete features, the numerical model was able to reproduce the characteristics of the temperature data in sensors both above and below the heater plane in TT1 and TT2.

The comparison of measured and simulated temperature in selected sensor locations around the time of the rain event for boreholes TT1 and TT2 is shown respectively in Figures 14 and 15. (Sensors numbered 1 through 13 are below the heater plane, and those numbered 15 through 28 are above the heater plane; Sensor TT1-14 is located at 0.05 m above, and Sensor TT2-14 is at 0.05 m below the heater plane). TH processes are clearly evident in the temperature data. Figure 14 shows that in borehole

TT1, cool rainwater bypasses some of the sensors above the heater plane, but once at the heater plane, the water rapidly vaporizes, accounting for the rapid drop in temperature at sensors TT1-14 (from approximately 140^{o}C to the boiling point of water) and TT1-16. On the other hand, the vertical high-permeability discrete feature intersecting the incline feature at TT1 provides a fast path for vapor to move upward, causing the temperature at the top of the block (TT1-28) to slowly increase from 60^{o}C to the boiling point of water over a period of approximately 30 hours.

Figure 15 shows that in TT2, the location of the vertical feature is such that rainwater causes a sharp drop in temperature (from the near-constant 60^{o}C prior to the rain event) in TT2-28 at the top boundary of the block. The signature of sharp drop in temperature followed by slow recovery becomes less prominent in successive sensors down the vertical hole. Sensor TT2-20 records virtually no change in temperature, indicating equilibrium between the below-boiling temperature at the sensor location and that of the rainwater reaching this location. TT2-14 and TT2-15, sensors that are much closer to the heater plane and that prior to the storm event have temperatures above boiling, exhibit cooling caused by the rainwater. Data and simulation also show that no falling liquid water reaches TT2-7, further below the heater plane.

The detailed discussion regarding the temperature reading of sensors at different locations above illustrates the utility of numerical modeling to study coupled processes. The processes of heating, vaporization, cooling, condensation, and liquid and gas flow, all acting in concert in the fractured rock, were inferred (understood) from the temperature data and the matching simulated results.

While heterogeneity is a key issue for understanding and predicting flow and transport in fractured rock, strongly heat-driven processes tend to average out the effects of small-scale heterogeneity, so that a continuum representation of the fractures often represents TH processes quite well. This is evidenced by the good agreement between data and model predictions for the Single Heater Test and Drift Scale Test, in which the fractures are given a homogeneous continuum representation, even though preheat air permeability measurements typically indicated permeability variability ranging over several orders of magnitude. Similarly, in the Large Block Test, fractures modeled as a homogeneous continuum can in general reproduce the temperature measurements (including heat-pipe signatures, indicating water and vapor counter flow). However, the storm event resulted in temperature data showing strong TH coupling that was attributable to flow in large, discrete features of scale comparable to the domain size of interest. Detailed mapping of the Large Block Test block confirmed the presence of several such discrete features. By superposing some of these discrete features onto the homogeneous fracture continuum in the dual-permeability representation of the fractured porous tuff, the TH processes associated with fast flow were deciphered.

IMPACT OF TH PROCESSES ON KEY REPOSITORY PERFORMANCE ISSUES

Thus far, we have focused on modeling as the key to a fundamental understanding of coupled TH processes in a fractured porous rock. To illustrate how a sound fundamental understanding is crucial for evaluating the performance of a geological repository in isolating the radioactive waste from the biosphere, we will here briefly discuss the impact of TH processes on two key repository performance issues.

Water Seepage into a Heated Emplacement Drift

In the unsaturated environment of the proposed repository site at Yucca Mountain, whether water can seep (and how much and how frequently) into the horizontal drifts (of diameter ~ 5 m) that host radioactive waste containers is key to waste container corrosion and mobilization of radionuclide transport. It was recognized in the early 1990s [*Buscheck and Nitao*, 1993a, 1993b, 1994] that heat generated from the radioactive decay of stored waste can have the positive effect of creating a zone of above-boiling temperature, thus keeping water away from the vicinity of the waste emplacement drift and potentially enhancing the natural system's ability to isolate the waste. However, it was also known that considerable uncertainties [*Pruess and Tsang*, 1994] were associated with the effectiveness of a vaporization barrier—rock with temperature above the boiling point of water turning liquid water into vapor—that would absolutely prevent liquid water from reaching the emplacement drifts. Uncertainties arise from issues such as future climate changes (leading to higher percolation fluxes reaching the drifts) and spatial heterogeneities in the fractured rock. All these issues have been revisited extensively in recent years, in preparation for the submittal of a License Application to construct the repository [2008, http://www.nrc.gov/waste/hlw-disposal/yucca-lic-app/yucca-lic-app-safety-report.html]. The great advance in computation capability in the last decade has allowed the Department of Energy's Yucca Mountain Project to address these issues in depth. In the following, we give a synopsis of these studies, and readers are referred to the cited publications for details.

Birkholzer et al. [2004a] describe numerical prediction of the coupled TH processes following waste emplacement in the proposed geologic repository for nuclear waste at Yucca Mountain, Nevada. A numerical model was developed to evaluate the potential for seepage into drifts in the presence of (1) the vaporization barrier (to water contacting radioactive waste) when temperatures around the drift are above the boiling point of water, and (2) the ever-present capillary barrier (at all temperatures) at the interface between the fractured porous rock and the open drift. The capillary barrier originates from the contrast of capillary forces between those in the rock (negative), and those of the drift opening (zero). The negative capillary forces in the rock imply that downward percolating water prefers to remain in the rock rather than enter into the drift, and that the water tends to be diverted around a drift opening. The drift opening thus constitutes a barrier, preventing water from seeping into the drift.

Heterogeneity in fracture permeability is important for seepage [*Birkholzer et al.*, 1999]. It gives rise to local permeability contrasts promoting channelized flow that may penetrate into the superheated rock zone, thus overcoming the vaporization barrier. Heterogeneity may also cause local saturation increases in the fractures close to the drift walls, thus overcoming the capillary barrier. Heterogeneity is incorporated within the numerical model [*Birkholzer et al.* 2004a], in that the fractures are conceptualized as a heterogeneous porous continuum, while the rock matrix is represented by a homogeneous continuum [*Haukwa et al*., 2003]. In addition, *Birkholzer and Zhang* [2006] developed a specific dual-permeability model where the interface area between the fracture and matrix continua is reduced to account for finger flow.

Birkholzer et al. [2004a] show that the thermal perturbation of the flow field is strongest during the first few hundred years after emplacement, corresponding to the period when rock temperature is highest and the vaporization barrier is most effective. Even with greatly increased downward flux from the condensation zone towards the drifts during this period, and at enhanced percolation fluxes—and in the presence of strong flow channeling because of small-scale fracture heterogeneity—model results still show that water cannot penetrate far into the superheated rock during the time that rock temperature is above boiling, and therefore no seepage enters the drifts. More recently, additional processes (such as natural convection of air flow within the drift) have been integrated into the TH processes within the fractured rock in the modeling of water seepage [*Birkholzer et al.,* 2006; 2008; *Danko et al*., 2008].

Because of the importance of the vaporization barrier to repository performance, and because the numerical simulation [*Birkholzer*, 2004a] implements a continuum representation for fractures that may underestimate the potential for preferential finger flow penetrating the above-boiling temperatures, *Birkholzer* [2003], *Birkholzer and Ho* [2003] and *Birkholzer et al.* [2004b], further investigated the effectiveness of the vaporization barrier, focusing attention on the discreteness of finger flow in fractures. *Birkholzer et al*. [2004b] examined in detail the distance a liquid finger is able to move through above-boiling-temperature rock before the water in the finger is completely vaporized, employing a semi-analytical approach. Results of this study demonstrate that finger flow is not able to penetrate through the superheated rock during the first several hundred years of repository heating (according the the current design of thermal load of 1.45 kW/m,), when rock temperature is high and boiling conditions exist in a sufficiently large region above the drifts. These are the conditions in which the largest thermal perturbation occurs, or, in other words, when the potential for episodic finger flow is highest. Only later, when the superheated zone is small and the impact of vaporization is limited, can water arrive at the drift crown. However, seepage of water into the drift is not expected from this limited water arrival, since the capillary barrier will still be in effect.

Repository Performance for Different Thermal Designs

Another example of how TH processes impact the repository performance is in their dependence on the repository thermal design. *Buscheck et al.* [1996] explored alternative repository thermal designs for using radioactive decay heat constructively. The thought was that heat would substantially reduce relative humidity and liquid flow near waste canisters for thousands of years, and thereby limit waste canister degradation and radionuclide dissolution and release. With a thermal load high enough, and a spacing between two adjacent emplacement drifts small enough, "extended dryout" can be achieved so that the drying of rock surrounding individual drifts coalesce, forming large-scale rock dryout. However, *Buscheck et al.* [1996] show that large-scale coalesced rock dryout also implies a large condensation zone above it, which might adversely affect waste isolation when the radioactive decay heat pulse passes and the temperature returns to ambient. Alternatively, a design using wide drift spacing and a thermal load too low for coalesced dry out would achieve "localized dryout". This design would reduce the possibility of condensate buildup above the drifts; it would, in fact, allow drainage of condensate in the pillars between adjacent emplacement drifts. The concept of "localized dryout" has been adopted in the current repository design for License Application

[*Civilian Radioactive Waste Management System (CRWMS)* , 1999a and 1999b], in which the spacing between emplacement drifts is 81 m instead of the much smaller 30 m drift spacing in earlier designs.

Buscheck et al. [2002; 2003] also employed a multiscale TH model to evaluate repository performance for different designs with respect to thermal design goals (e.g. keeping waste containers dry). In the locally boiling or globally boiling thermal design under consideration, a considerable volume of rock mass around the emplacement drifts would be above the boiling point of water for hundreds to thousands of years. In the sub-boiling thermal design, the host rock temperature would be below the boiling point everywhere and at all times. This multiscale modeling approach [*Buscheck et al*., 2002; 2003] meets the objective of simultaneously accounting for processes occurring at the scale of a few tens of centimeters around individual waste containers within emplacement drifts, and at the multikilometer scale of the mountain. A number of simplifying assumptions were made to employ this model as a cost-effective numerical tool for conducting a large number of realizations. These assumptions include the following: (1) the fully coupled TH processes are implemented in only two dimensions on the drift scale; (2) only heat conduction is included on the mountain scale; and (3) the in-drift processes are not fully coupled to the in-rock processes. This multiscale model was used to evaluate repository performance with respect to a number of design options, with a range of values for the associated thermal design parameters. *Buscheck et al.* [2002; 2003] simulate the in-drift TH conditions (specifically, temperature and relative humidity) in representative host-rock repository units, with selected locations accounting for the effect of repository-edge cooling for different waste container types and emplacement options. Temperature and humidity parameters within the waste emplacement drifts are controlling factors on the potential for waste container corrosion, and in turn repository performance.

RECENT ADVANCES AND FUTURE RESEARCH DIRECTIONS

This review has focused on the study of TH processes within the rock. More recently, it has become evident that TH processes within the drift in which waste containers are placed also play an important role in the performance of a repository. Developing models to study the TH processes within drift and how they relate to that within the rock mass in a fully coupled framework is one of the more recent research advances [*Danko,* 2006*; Danko et al.*, 2008].

Research on thermally driven coupled-processes in the rock has historically centered on the TH processes, because they constitute the most prominent and direct impact on flow and transport. More recently, however, investigators have begun incorporating chemical [*Xu et al.*, 2001; *Spycher et al*., 2003; *Xu et al.*, 2004; *Sonnenthal et al*., 2005, *Mukhopadhyay et al.*, 2006] and mechanical [e.g*., Rutqvist et al.*, 2002; *Rutqvist and Tsang,* 2003; *Rutqvist et al.*, .2004; 2005], processes into the thermally driven hydrological processes, within a coupled modeling framework.

In-Drift and In-Rock Thermal-Hydrological Processes

While the radioactive decay of the nuclear waste placed in the drifts heats up the rock mass, the open drifts will act as important conduits for natural convection and ventilation processes. For example, as a result of natural convection driven by in-drift axial temperature gradients, water will evaporate from the drift walls in elevatedtemperature sections of the drifts, migrate along the drifts, and condense in cooler sections. Evaporation driven by natural convection may significantly reduce the moisture content in the near-drift fractured rock, which in turn can reduce the potential for seepage of water into the drift. *Danko* [2006] developed a numerical code, MULTIFLUX, to simulate the heat and moisture flows within the drift. MULTIFLUX describes the velocity distribution in the drift air space, and the transport of heat and moisture by laminar or turbulent convection in the in-drift domain with a lumped-parameter CFD (Computational Fluid Dynamics) modeling approach. It also provides an efficient iterative coupling technique for matching the mass and heat transfer between the drift and the rock mass, in a fully coupled framework [*Danko et al*., 2008].

This newly developed approach has been applied to evaluate how the heat-driven flow and transport processes in and near a representative waste emplacement drift impact the performance of the repository at Yucca Mountain. Given that the majority of research on TH processes (subject of this review) focus on the rock mass, and treat the drift as a boundary, the MULTIFLUX model affords a future research opportunity to reexamine many in-rock phenomena, such as seepage into the emplacement drift, by taking account of the in-drift TH processes explicitly.

Thermal-Hydrologic-Chemical Processes

These processes, in the context of the drift setting at Yucca Mountain [*Spycher et al.,* 2003; *Sonnenthal et al.*, 2005], take into account water-gas-rock interactions, the transport of aqueous and gaseous species, and mineralogical characteristics and changes, all within a heated, unsaturated, fractured rock environment. The chemical evolution of waters, gases, and minerals is intimately coupled to the thermal-hydrological processes (boiling, condensation, and drainage). Condensate distribution within the fracture system determines where mineral dissolution and precipitation can occur in the fractures, and where there can be direct interaction (via diffusion) between matrix pore waters and fracture waters. Figure 16 schematically shows the relationships between thermal hydrologic and geochemical processes in the zones of boiling, condensation, and drainage in the rock mass at a fracture-matrix interface outside the drift and above the heat source. With an increase in temperature, dissolved CO_2 will degas from the water, the exsolution of CO_2 in the boiling zone results in a local increase in pH, as well as a decrease in pH within the condensation zone into which the vapor-enriched CO_2 is transported and condensed. Because the diffusivities of gaseous species are several orders of magnitude greater than those of aqueous species, and because the advective transport of gases (occurring predominantly in fractures) can be more rapid than that of liquids, the region where CO_2 degassing affects water and gas chemistry could be much larger than the region affected by the transport of aqueous species.

The effects of thermal hydrologic processes on water chemistry are varied. They depend on the behavior of the dissolved species and their relation to mineral-water reactions. Nonreactive and nonvolatile species, such as chloride, become concentrated in waters undergoing vaporization or boiling, but are essentially absent from the vapor condensing in the fractures. The concentrations of more reactive aqueous species, such as calcium, are also affected by mineral dissolution or precipitation reactions, and by exchange or alteration reactions involving Ca-bearing zeolites, clays, or feldspars.

Zonation in the distribution of mineral phases in both the condensation and boiling zones (displayed in Figure 16) can occur as a result of differences in mineral solubility as a function of temperature. Calcite ($CaCO_3$), the major mineral in the fractures throughout the repository block, is less soluble with increasing temperature, while most other minerals, such as silica, are more soluble at higher temperatures.

Amorphous silica and calcite precipitates result in long-term permeability reduction of the surrounding fractured rock. Evaporative concentration also results in the precipitation of gypsum (or anhydrite), halite, fluorite, and other salts. These evaporative minerals eventually redissolve after the boiling period is over; however, their precipitation results in a significant temporary decrease in permeability. Reduction of permeability is also associated with changes in fracture capillary characteristics. In short, the coupled thermal-hydrologic-chemical processes dynamically alter the hydrological properties of the rock. The feedback of the thermal-chemical processes on the hydrologic properties of the unsaturated fractured host rock has been considered in recent studies [*Mukhopadhyay et al*., 2006*; Mukhopadhyay et al*., 2007a; *Mukhopadhyay et al*., 2007b]. These studies show that the feedback of thermal-chemical processes on fracture hydraulic properties can significantly impact the local flow channeling and amount of seepage.

Thermal-Hydrologic-Mechanical Processes

Table 2 shows the potential couplings between thermal, hydrological, and mechanical processes in geological media for a matrix of parameters. The three diagonal elements of the matrix represent respectively the fundamental thermal, hydrological, and mechanical parameters. The off-diagonal elements denote the parameters in the "column" process impacted by the “row” process. For example, the element of Row 1 and Column 3 shows that thermal processes affect the mechanical processes in the thermal expansion of the rock mass. The expansion leads to thermal strain, and since in a confined rock-mass environment, the rock material cannot expand freely, thermal stress can occur. Conversely, mechanical processes may affect thermal processes in the conversion of mechanical energy to heat; or thermal conductivity through mechanically induced changes in porosity. However, both these are expected to be negligible in the context of geological nuclear waste disposal. Mechanical energy conversion is only significant in very special cases (say, from large-scale fault slip during major earthquakes). The thermal conductivity of rock is predominantly controlled by the thermal conductivity of the rock matrix—and in lithophysal-rich rock units, also by the lithophysal porosity. The porosity of rock matrix and the lithophysal cavities is not expected to be significantly altered by the typical magnitudes of thermally induced stresses at a geological repository. For this reason, the off-diagonal matrix element corresponding to Row 3, Column 1 is labeled N/A.

Table 2 also shows that mechanical processes can impact hydrological processes through mechanically induced changes in porosity and permeability. Conversely, hydrological processes can affect mechanical processes through fluid-pressure-induced changes in “effective stress” or through moisture-induced swelling of the geological material. The latter is expected to be negligibly small. On the other hand, the coupling from mechanical processes to hydrological processes for thermal-mechanically-induced changes in porosity and permeability is important [*Rutqvist et al*., 2005].

Future Research

While study of in-rock TH processes and their applications has become a mature research area over the last three decades, the coupling of chemical and mechanical processes to thermal hydrologic phenomena, as outlined in the above sections, is still in its developmental stage, offering opportunities for further research. Investigations in these areas will be relevant not only to the geological disposal of radioactive waste, but also to the geological sequestration of CO_2 and development of geothermal energy, both of which are vitally important applications for earth sciences research in the 21st century.

Furthermore, though it is generally recognized that microbes play an important role in regulating geochemical cycles, there is relatively little understanding of the mechanisms by which the microbial community interact with the geochemical environment. Current microbial-biogeochemical models for reactive transport lack a suitable mechanistic treatment of these processes at the cellular level. The often-empirical approach greatly hampers our ability to predict behavior under a range of conditions and environments. Therefore, biogeochemistry of the subsurface geological environment will be fertile ground for much fundamental research, both experimental and modeling.

CONCLUSION

We have reviewed the research that has led to a better understanding of flow and transport processes under strong heat stimulation in fractured porous rock. Advances in this area of coupled processes research were propelled by the urgent need for a sound scientific basis in the safety evaluation of a geological repository for the disposal of high-level radioactive waste. We started with defining the physical problem, describing the anticipated phenomena in a partially saturated fractured rock when the physical processes of heat conduction, heat convection, phase changes, and gas and liquid flow act in concert with one another. We gave the rationale for numerical modeling being the key element to study thermal hydrological processes that are coupled. The paper described the evolution of the conceptual and numerical model, progressing from the simplified to the more realistic.

The chief characteristics of the numerical modeling applied to *in situ* field thermal tests beginning in the late 1990s are: (1) incorporation of a full set of TH processes into a numerical simulator, eliminating the need for simplifying assumptions because of computational constraints; (2) realistic representation of the field test geometry, in three-dimensions if warranted; and (3) use of site-specific characterization data for model inputs. Model predictions were carried out prior to initiation of data collection, and the modeled results were compared with diverse sets of measurements. Such a close integration between sophisticated modeling and field test measurements has greatly increased our understanding of the multiple thermal, hydrological, chemical, and mechanical processes that come into play in a partially saturated, fractured porous volcanic geological formation—when it is subject to a heat source such as that from the decay of radionuclides in a nuclear waste repository. This review focused on modeling the TH aspects of the coupled processes. The coupling of chemical, mechanical processes to flow and transport processes should remain active areas of research in the years to come. Incorporating microbiological processes into the strongly heat-driven coupled-processes system has scarcely been attempted—and would provide rich opportunities for fundamental research.

APPENDIX A—Mathematical Formulations for TH Processes

The basic mass- and energy-balance equations solved can be written in the general form [*Pruess*, 1991; *Pruess et al.*, 1999]

$$\frac{d}{dt}\int_{V_n} M^{\kappa}\, dV_n = \int_{\Gamma_n} \boldsymbol{F}^{\kappa}\boldsymbol{n}\; d\Gamma_n + \int_{V_n} q^{\kappa} dV_n \tag{A1}$$

The integration is over an arbitrary subdomain V_n of the TH system under study, which is bounded by the closed surface Γ_n. The quantity M appearing in the accumulation (left hand side) represents mass or energy per volume, with $\kappa = 1, 2$ labeling the mass components water and air, and $\kappa = 3$ the "heat component." F denotes mass or heat flux (see below), q denotes sinks and sources, and n is a normal vector on surface element $d\Gamma_n$, pointing inward into V_n.

The general form of the mass accumulation term is

$$M^{\kappa} = \phi\sum_{\beta} S_{\beta}\rho_{\beta}X_{\beta}^{\kappa} \tag{A2}$$

The total mass of component κ is obtained by summing over the phases β (= liquid, gas), with ϕ the porosity, S_β the saturation of phase β (i.e., the fraction of pore volume occupied by phase β), ρ_β the density of phase β, and X_{β}^{κ} the mass fraction of component κ in phase β. Similarly, the heat accumulation term in a multiphase system is

$$\boldsymbol{M}^{3} = (1-\phi)\rho_{\boldsymbol{R}}\boldsymbol{C_R T} + \phi\sum_{\beta}\boldsymbol{S}_{\beta}\rho_{\beta}\boldsymbol{u}_{\beta} \tag{A3}$$

where ρ_R and C_R are, respectively, rock-grain density and specific heat capacity of the rock, T is temperature, and u_β is specific internal energy in phase β. Note that this formulation is based on accumulation of internal energy, rather than on accumulation of specific enthalpy [*Nitao*, 2000]. This simplification is valid for all TH systems where the energy associated with volumetric changes in the gas phase, caused by pressure changes, is small compared to the energy associated with temperature changes. For the fractured rock at Yucca Mountain, this condition is justified, and the distinction between enthalpy and internal energy of the gas phase can be neglected.

Advective mass flux is a sum over phases,

$$\boldsymbol{F}^{\kappa}\Big|_{adv} = \sum_{\beta} X_{\beta}^{\kappa} \boldsymbol{F}_{\beta}, \tag{A4}$$

And individual phase fluxes are given by a multiphase version of Darcy's law (continuum representation),

$$\mathbf{F}_{\beta} = \rho_{\beta}\mathbf{u}_{\beta} = -\boldsymbol{k}\frac{\boldsymbol{k}_{r\beta}\rho_{\beta}}{\mu_{\beta}}\left(\nabla \boldsymbol{P}_{\beta} - \rho_{\beta}\mathbf{g}\right) \tag{A5}$$

Here, $\mathbf{u}_{\beta}$ is the Darcy velocity in phase β, k is absolute permeability, $k_{r\beta}$ is the relative permeability to phase β, μ_{β} is viscosity, and

$$P_{\beta} = P + P_{c\beta} \tag{A6}$$

is the fluid pressure in phase β, which is the sum of the pressure P of a reference phase (gas pressure) and the capillary pressure $P_{c\beta}$ (≤ 0); and g is the vector of gravitational acceleration. Vapor-pressure lowering is modeled by Kelvin's equation:

$$P_v(T,S_l) = f_{vpl}(T,S_l)\ P_{sat}(T) \tag{A7}$$

where

$$f_{vpl} = exp\left[\frac{M_w P_{cl}(S_l)}{\rho_l R(T + 273.15)}\right] \tag{A8}$$

is the vapor-pressure lowering factor, identical to the definition of relative humidity. P_{sat} is the saturated vapor pressure of the bulk liquid phase, P_{cl} is the difference between liquid and gas phase pressure, M_w is the molecular weight of water, and R is the universal gas constant. Vapor-pressure lowering is a well-known physical process that allows for the presence of liquid water in small rock pores at temperatures above the nominal boiling point.

Heat flux includes conductive and convective components:

$$\boldsymbol{F}^3 = -\lambda \nabla T + \sum_\beta h_\beta F_\beta \tag{A9}$$

where λ is the thermal conductivity of the rock-fluid mixture, and h_β is the specific enthalpy in phase β.

The transport equations given above are complemented with constitutive relationships, which express all parameters as a function of a set of primary variables. In TOUGH2 [*Pruess*, 1991; *Pruess et al.*, 1999], the thermophysical properties of water substance are accurately described by the steam table equations, as given by the *International Formulation Committee* [1967]. Air is approximated as an ideal gas, and gas pressure is the sum of the partial pressures for air and vapor. The solubility of air in liquid water is calculated from Henry's law.

Capillary pressures and relative permeabilities depend on phase saturation. For liquid, the capillary suction and the relative permeability have the van Genuchten functional forms [*van Genuchten*, 1980; *Mualem*, 1976]:

$$P_{cl} = -\frac{1}{\alpha}\left[\left(S_{l,eff}\right)^{-1/m} - 1\right]^{1-m}$$

$$k_{rl} = \left(S_{l,eff}\right)^{1/2}\left[1-\left(1-\left(S_{l,eff}\right)^{1/m}\right)^{m}\right]^{2} \tag{A10}$$

$$S_{l,eff} = \frac{\left(S_{l}-S_{lr}\right)}{\left(1-S_{lr}\right)}$$

where $S_{l,eff}$ is liquid effective saturation, S_l is liquid saturation, S_{lr} is liquid residual saturation, and m and $1/\alpha$ are fitting parameters, the latter related to the capillary strength of the medium.

At very small saturation close to the residual saturation value, the van Genuchten capillary pressure function approaches infinity. This can lead to nonphysical, extremely high capillary-pressure values, particularly in areas with strong heating and dryout of water close to or even below residual. Therefore, at saturation below a given small threshold value, a linear capillary pressure function is applied instead of the above power function. The slope of this linear function is determined by the slope of the van Genuchten equation at the threshold saturation value.

Relative permeability for gas flow is described by the modified *Brooks and Corey* [1966] formulation, as follows:

$$k_{rg} = \left(1-S_{l,eff}\right)^{2}\left(1-\left(S_{l,eff}\right)^{\frac{2+p}{p}}\right), \tag{A11}$$

where $p = m/(1\text{-}m)$. The selected formulations for the dependence of the capillary pressure and the relative permeability on liquid-phase saturation are widely employed in the literature.

The thermal conductivity of the rock matrix is calculated using a square-root interpolation between dry and wet conductivities as a function of liquid saturation:

$$\lambda(S_l) = \lambda_{dry} + (\lambda_{wet} - \lambda_{dry})\sqrt{S_l} \tag{A12}$$

This square-root relationship is commonly used in the literature [*Pruess*, 1987]. The resulting thermal conductivity represents the rock matrix plus fluid system.

In the TOUGH2 simulator [*Pruess 1991*; *Pruess et al*., 1999], the continuum balance equations are discretized in space using the integral finite-difference approach, and time is discretized as fully implicit. The discretized balance equations are written in terms of residuals (difference in the primary variables between two successive iteration steps at all space locations), and iteration is continued until the residuals are reduced below a preset convergence tolerance. If convergence cannot be achieved within a certain number of (default or user supplied) iterations, the time step size is automatically reduced and a new iteration process is started. This ensures adequate time-stepping control without compromising accuracy.

ACKNOWLEDGMENT

This manuscript has been authored by Lawrence Berkeley National Laboratory under Contract No. DE-AC02-05CH11231 with the U.S. Department of Energy. The views and opinions of authors expressed in this article do not necessarily state or reflect those of the United States Government or any agency thereof or The Regents of the University of California.

REFERENCE LIST

Alonso, E.E. and J. Alcoverro (2003), The FEBEX benchmark test case definition and composition of different modeling approaches, Proceedings, GeoProc 2003, an International conference on Coupled T-H-M-C processes in Geo-systems: Fundamentals. Modeling, Experiments & Applications, Royal Institute of Technology, Stockholm, Sweden, 13-15 October.

Barenblatt, G. E., I. P. Zheltov, and I. N. Kochina (1960), Basic concepts in the theory of seepage of homogeneous liquids in fissured rocks, *J. Appl. Math. (USSR), 24*, 1286-1303.

Birkholzer, J. T. (2003), Penetration of liquid fingers into superheated fractured rock, *Water Resour. Res.*, *39(4)*, 9-1 through 9-21.

Birkholzer, J.T. (2006a), A temperature-profile method for estimating flow in geologic heat pipes, *Journal of Contaminant Hydrology, 85*, pp. 89-117.

Birkholzer, J.T. (2006b): Estimating liquid fluxes in thermally perturbed fractured rocks using measured temperature profiles, *Journal of Hydrology, 327*, pp. 496-515.

Birkholzer, J.T., N. Halecky, S.W. Webb, P. F. Peterson, and G.S.Bodvarsson (2008), A modeling study evaluating the thermal-hydrological conditions in and near waste emplacement tunnels at Yucca Mountain, *Journal of Nuclear Technology*, *163(1),* pp. 147-164.

Birkholzer, J.T., G. Li, C.-F. Tsang, and Y.W. Tsang (1999), Modeling studies and analysis of seepage into drifts at Yucca Mountain. *J. Contam. Hydrol. 38(1-3)*, 349-384.

Birkholzer, J.T., C.K. Ho (2003), A probabilistic analysis of episodic preferential flow into superheated fractured rock, *Journal of Hydrology, 284*, pp.151-173.

Birkholzer, J., S. Mukhophadhyay, and Y. W. Tsang (2004a), Modeling seepage into heated waste emplacement tunnels in unsaturated fractured rock, *Vadose Zone Journal*, *3*, 819–836.

Birkholzer, J., S., S. Mukhophadhyay and Y. W. Tsang (2004b), The impact of preferential flow on the vaporization barrier above waste emplacement drifts at Yucca Mountain, *Nuclear Technology 148*, 138-150.

Birkholzer, J.T., and Y.W. Tsang (1997), Pretest analysis of the thermal hydrological conditions of the ESF Drift Scale Test, *Rep. LBNL-41044*, Lawrence Berkeley National Laboratory, Berkeley, CA.

Birkholzer, J.T., and Y.W. Tsang (2000), Modeling the thermal-hydrologic processes in a large scale underground heater test in partially saturated tuff, *Water Resour. Res., 36(6)*, 1431-1447.

Birkholzer, J.T., S.W. Webb, N. Halecky, P.F. Peterson, G.S. Bodvarsson (2006): Evaluating the Moisture Conditions in the Fractured Rock at Yucca Mountain – The Impact of Natural Convection in Heated Emplacement Drifts, *Vadose Zone Journal, 5*, pp. 1172-1193.

Birkholzer, J.T.and Y. Zhang (2006), The Impact of Fracture-Matrix Interaction on Thermal-Hydrological Conditions in Heated Fractured Rock, *Vadose Zone Journal, 5*, pp. 657-672.

Bixler, N.E. (1985), NORIA−A finite element computer program for analyzing water, vapor, air and enegy tranposrt in porous media, *Rep. SAND84-2057*, Sandia National Laboratories, Albuquerque, NM.

Brooks, R.H., and A.T. Corey (1966), Properties of porous media affecting fluid flow, *Journal of the Irrigation and Drainage Division, Proceedings of the American Society of Civil Engineers*, 92, (IR2), 61-89. Ann Arbor, Michigan.

Buscheck. T. A., and J. J. Nitao (1991), Modeling hydrothermal flow in variably saturated, fractured, welded tuff during the prototype engineered barrier system field test of the Yucca Mountain Project, *Technical Report UCRL-JC-106521*, Lawrence Livermore National Laboratory, Livermore CA.

Buscheck, T.A., and J.J. Nitao (1993a), The analysis of repository-heat-driven hydrothermal flow at Yucca Mountain, *Proceedings of the Fourth Annual International Conference on High Level Radioactive Waste Management, (1)* pp. 847–867, Las Vegas, Nevada, April 26–30.

Buscheck, T.A., and J.J. Nitao (1993b), Repository-heat-driven hydrothermal flow at Yucca Mountain, part 1: Modeling and analysis. *Nuclear Technology, 104,* 418–448.

Buscheck, T.A., and J.J. Nitao (1994), The impact of repository heat on hydrological behavior at Yucca Mountain. *UCRL-JC-115798*, Livermore CA, Lawrence Livermore National Laboratory.

Buscheck, T.A., J. J. Nitao, and L. D. Ramspott (1996), Localized dryout: An approach for managing the thermal-hydrological effects of decay heat at Yucca Mountain, in *Scientific Basis for Nuclear Waste Management XIX, Materials Research Society Symposium Proceedings, 412*, edited by W. M. Murphy and D. A. Knecht, pp.715–722, Materials Research Society, Pittsburgh, PA.

Buscheck, T. A. (1998), Thermal hydrological models, Technical Report UCRL-ID-131007, Lawrence Livermore National Laboratory, Livermore, California.

Buscheck, T. A., N. D. Rosenberg, J. Gansemer, and Y. Sun (2002), Thermohydrologic behavior at an underground nuclear waste repository, *Water Resour. Res., 38 (3),* 1028.

Buscheck, T.A., N. D. Rosenberg, J.A. Blink, Y. Sun, and K. Mansoor (2003), Analysis of thermohydrologic behavior for above-boiling and below-boiling thermal-operating modes for a repository at Yucca Mountain, *J. Contam. Hydrol*., *62–63*, 441–458.

Chijimatsu, M., T. Fujita, Y. Sugita, K. Amemiya, A. Kobayashi (2001), Field experiment, results and THM behavior in the Kamaishi mine experiment. *Int. J Rock Mech. Min. Sci*. 38(1), 67-78.

Cook, N.G. W. and M. Hood (1978), Full-scale and time-scale heating experiments at Stripa: Preliminary results, *Report LBL-7072*, Lawrence Berkeley National Laboratory, Berkeley, CA.

Cook, N.G.W., P. A. Witherspoon (1978), Mechanical and thermal design considerations for radioactive waste repositories in hard rock, *Technical Report LBL-7073, SAC-10*, Lawrence Berkeley National Laboratory, Berkeley, CA.

Civilian Radioactive Waste Management System (CRWMS) (1999a), License application design selection report, B00000000-01717-4600-00123, Rev. 01ICN01, , CRWMS Management and Operating Contractor (M&O),Las Vegas, Nev.

Civilian Radioactive Waste Management System (CRWMS) (1999b), Enhanced design alternative II report, B00000000-01717-5705-00131, REV. 00, CRWMS Management and Operating Contractor (M&O), Las Vegas, Nev.

Civilian Radioactive Waste Management System (CRWMS) (2000), Thermal tests thermal-hydrological analyses/model report, ANL-NBS-TH-000001 REV 00, CRWMS Management and Operating Contractor (M&O), Las Vegas, Nev.

Danko, G.; H. Creech; J. Phillips.; and S.Tippabhatla (1998). In Situ Reka Probe Measurements at Fran Ridge and in the ESF at Yucca Mountain. *Proceedings, Eighth International High-Level Radioactive Waste Management Conference*, Las Vegas, NV, 54–56. La Grange Park, IL: American Nuclear Society.

Danko, G. and P. F. Mousset-Jones (1991). A probe method for measuring in situ thermophysical properties, *Proceedings, 2nd International High Level Radioactive Waste Management Conference, Las Vegas, NV, April 28–May 3, 1991*, 555–563. La Grange Park, IL: American Nuclear Society.

Danko, G., (2006), Functional or operator representation of numerical heat and mass transport models, *ASME J. of Heat Transfer, Vol. 128*, pp. 162-175.

Danko, G., J.T. Birkholzer, D. Bahrami, (2008), Coupled in-Rock and in-Drift Hydrothermal Model Study for Yucca Mountain, *Journal of Nuclear Technology*, 163 (1), pp. 110–128.

DOE (2002), Final environmental impact statement for a geologic repository for the disposal of spent nuclear fuel and high-level radioactive waste at Yucca Mountain, Nye

County, Nevada. *DOE/EIS-0250*, U.S. Department of Energy, Office of Civilian Radioactive Waste Management, Washington, D.C.

Doughty, C. (1999), Investigation of conceptual and numerical approaches for evaluating moisture, gas, chemical, and heat transport in fractured unsaturated rock, *J. Cont. Hydro., 38 (1–3)*, 69–106.

Eastman, G.Y. (1968), The heat pipe, *Sci, Am., 218(5)*, 38–46.

Edwards, A. L. (1972), TRUMP: A computer program for transient and steady state temperature distributions in multidimensional systems. National Technical Information Service, National Bureau of Standards, Springfield VA.

Flint, L.E. (1998), Characterization of hydrogeologic units using matrix properties, Yucca Mountain, Nevada, *Water Resources Investigation Report 97-4243*, U.S. Geologic Survey, Denver, CO.

Gregory, E.C. and K. Kim (1981), Preliminary results from the full-scale heaters tests at the near-surface test facility. *Proceedings of the 22nd U.S. Rock Mechanics Symposium*, pp. 143-148, 29 June-2 July 1981, Massachusetts Institute of Technology, Cambridge, MA.

Ghezzehei, T.A., and H.H. Liu (2004), Calibrated Properties Model, MDL-NBS-HS-000003 REV 02, Bechtel SAIC Company, Las Vegas, NV

Gros, J.C. and A. Rejeb (1995), Participation to the International co-operative DECOVALEX Project, Modelling of THM behavior for fractured rocks, *CEC report, Nuclear Science and Technology, EUR 16219 EN.*, pp 177-209, Brussels, Belgium.

Hardin, E. L. (1998), Near field/altered zone models report, Technical Report UCRL-ID-129179, Lawrence Livermore National Laboratory, Livermore, California.

Haukwa, C.B., Y.W. Tsang, Y.-S. Wu, and G. S. Bodvarsson (2003), Effect of heterogeneity on the potential for liquid seepage into heated emplacement drifts on the potential repository, *J. Contam. Hydrol. 62–63*, 509–527.

Huang, K., Y.W. Tsang, and G. S. Bodvarsson (1999), Simultaneous inversion of air-injection tests in fractured unsaturated tuff at Yucca Mountain, *Water Resour. Res.*, *35*, 2375-2386.

International Formulation Committee (1967), The 1967 IFC Formulation for Industrial Use, A Formulation of the Thermodynamic Properties of Ordinary Water Substance, Düsseldorf, Germany: International Formulation Committee of the Sixth International Conference on the Properties of Steam.

Lieb, W. (1988), The Grimsel Test Site from 1983 to 1990 – An Overview, *Nagra Bulletin. 5-13* (Special Edition 1988 [English]), Wettingen, Switzerland.

Lin, W., S.C. Blair, D. Wilder, S. Carlson, J. Wagoner, L. Deloach, G. Danko, A.L. Ramirez, and K. Lee (2001), Large Block Test Final Report, *Tech. Rep.UCRL-ID-132246, Rev.2.* Lawrence Livermore National Laboratory, Livermore, CA.

Martino, J. B. and R. S. Read (1994), Mine-by-Experiment Phase III-Heated Failure Tests, Technical Progress Report and Summary of State 1. Atomic Energy of Canada *(AECL) Report TR-652, COG-94-478, URL-EXP-022-R32*, Whiteshell Laboratories, Pinawa, Canada.

Majer, M. L., and T. V. McEvilly (1985), Acoustic emission and wave propagation monitoring at the spent fuel test: Climax, Nevada. *Int. J. Rock Mech. Min. Sci. & Geomech. 22 (4)*, 215-226.

Metalucci, R.V., C.L. Christensen, T. O. Hunter, M. A. Molecke, and D. E. Munson (1982), Waste isolation Pilot Plant (WIPP) research and development program: In situ NM.

Miller, J.D., and D.W. Allman (1986), Dual permeability modeling of flow in a fractured geothermal reservoir, *Proceedings, Eleventh Workshop on Geothermal Reservoir Engineering*, pp.77–84, Stanford University, Stanford, CA.

Mondy, L. A., R. K. Wilson, and N. E. Bixler (1983), Comparison of waste emplacement configurations for a nuclear waste repository in tuff—IV. Thermohydrological analysis, *Rep. SAND83-0757*, Sandia National Laboratories, Albuquerque, NM.

Mualem, Y. (1976), A new model for predicting the hydraulic conductivity of unsaturated porous media, *Water Resources Research*, 12, (3), 513-522.

Mukhopadhyay, S., E.L. Sonnenthal, and N. Spycher (2006), Modeling coupled thermal-hydrological-chemical processes in the unsaturated fractured rock of Yucca Mountain, Nevada: heterogeneity and seepage, *Physics and Chemistry of the Earth*, 31, 626-633, doi: 10.1016/j.pce.2006.04.018, 2006.

Mukhopadhyay, S., E.L. Sonnenthal, and N. Spycher (2007a), Modeling of coupled heat transfer and reactive transport processes in porous media: Application to seepage studies at Yucca Mountain, Nevada, presented in the *Second International Conference on Porous Medium and its Applications in Science, Engineering, and Industry, Kauai, HI*, June 17-21, 2007.

Mukhopadhyay, S., N. Spycher, G.X. Zhang, E.L. Sonnenthal, and S. Finsterle (2007b), THC sensitivity study of heterogeneous permeability and capillarity effects, *ANL-NBS-HS-000047 REV 01*, Sandia National Laboratories, OCRWM Lead Laboratory for Repository Systems, Las Vegas, Nevada.

Mukhopadhyay S., and Y.W. Tsang (2002), Understanding the anomalous temperature data from the large block test at Yucca Mountain, Nevada, *Water Resour. Res., 38* (10), 1210, doi: 10.1029/2001WR001059.

Mukhopadhyay, S., and Y.W. Tsang (2003), Uncertainties in coupled thermal-hydrological processes associated with the Drift Scale Test at Yucca Mountain, Nevada, *J. Contam. Hydrol., 62–63*, 595–612.

Munson, D. E., R.L. Jones, D.L. Hoag, J.R. Ball (1988), Heated Axisymmetric Pillar Test (Room H): In Situ Data Report (February 1985-April 1987) Waste Isolation Pilot Plant

(WIPP) Thermal/Structural Interaction Program *SAND88-1460*, Sandia National Laboratories, Albuquerque, NM.

Munson, D. E., R.L. Jones, D.L. Hoag, J. R. Ball, R. M. Clancy and S.V. Petney (1989), Overtest for simulated defense high-level waste (Room B) in situ data report (May 1984-February 1989), *SAND89-2671*, Sandia National Laboratories, Albuquerque, NM.

Narasimhan, T.N., P. A. Witherspoon (1976), An integrated finite difference method for analysizaing fluid flow in porous media, *Water Resour. Res. (12)*, 57-64.

National Academy of Sciences – National Research Council (1957), The disposal of radioactive waste on land. Report of the Committee on Waste Disposal of the Division of Earth Sciences, *Publication 519*, National Academy of Sciences, Washington, D. C.

Nitao, J.J. (1993), The NUFT Code for modeling nonisothermal, multiphase, multicomponent flow and transport in porous media, In proceedings from EOS. Washington, DC.: American Geophysical Union.Supplement 73:31.

Nitao, J.J. (1995). Reference manual for the NUFT flow and transport code, Version 1.0. Technical Report UCRL-IC-113520, Lawrence Livermore National Laboratory, Livermore, CA:.

Nitao, J.J. (1998). Reference manual for the NUFT flow and transport code, Version 2.0. Technical Report *UCRL-MA-130651*, Lawrence Livermore National Laboratory, Livermore, CA:.

Nitao, J.J. (2000), Documentation of the thermal energy balance equation used in the USNT Module of the NUFT flow and transport Code, *UCRL-ID-139836*, Lawrence Livermore National Laboratory, Livermore, CA.

Noynaert, L., G. Volckaert and P. De Cannière (1995), The thermo-hydro-mechanical aspects of the CERBERUS test: experimental results and preliminary modeling. CEC report, *Nuclear Science and Technology, EUR 16219 EN.*, pp. 17-31, Brussels, Belgium.

Patrick, W.C. (1986), Spent fuel test-Climax: An evaluation of the technical feasibility of geological storage of spent nuclear fuel in granite, final report, *Report UCRL- -53702*, Lawrence Livermore National Laboratory, Livermore, CA.

Peters, R.R., and E.A. Klavetter (1988.), A continuum model for water movement in an unsaturated fractured rock mass, *Water Resour. Res.,* 24(3), 416–430.

Picard, J.-M., B. Bazargan, G. Rousset, B. Vignal (1991), Behavior of Boom Clay under thermal loading: First results from CACTUS 1 in situ Test. *CEC report, Nuclear Science and Technology*, EUR 13985 En. pp.255-264.

Picard., J.-M., B. Bazargan, G. Roussett, F. Plas (1995), The CACTUS in situ tests. CEC report, *Nuclear Science and Technology, EUR 16219 EN.*, pp. 51-61, Brussels, Belgium.

Polluck, D.W. (1986), Simulation of fluid flow and energy transport processes associated with high-level radioactive waste disposal in unsaturated alluvium, *Water Resour. Res., 22(5)*, 765–775.

Pruess, K. (1987), TOUGH user's guide. *Rep. LBL-20700,* Lawrence Berkeley National Laboratory, Berkeley, CA.

Pruess, K. (1991), TOUGH2: A general purpose numerical simulator for multiphase fluid and heat flow, *Technical Report LBL-29400, UC-251*, Lawrence Berkeley National Laboratory, Berkeley, CA.

Pruess, K., C. Oldenburg and G. Moridis (1999), TOUGH2 user's guide, Version 2.0, *Technical Report LBNL-43134*, Lawrence Berkeley National Laboratory, Berkeley, CA.

Pruess, K., Y.W Tsang, and J.S. Y. Wang (1985), Modeling of strongly heat-driven flow in partially saturated fractured porous media, *Memoires, 17*, 486–497, International Association of Hydrogeologists, Arnhem, The Netherlands.

Pruess, K., and Y. Tsang (1994), Thermal modeling for a potential high-level nuclear waste repository at Yucca Mountain, *Technical Rep. LBL-35381*, Lawrence Berkeley National Laboratory, Berkeley, CA

Pruess K., and J.S.Y. Wang (1984), TOUGH-A numerical model for nonisothermal unsaturated flow to study waste canister heating heating effects, in *Scientific Basis for Nuclear Waste Management, Mat. Res. Soc. Symp. Proc., 26*, G. L. McVay, ed., pp. 1031–1038, Elsevier, New York.

Pruess, K., and J.S.Y. Wang (1987), Numerical modeling of isothermal and nonisothermal flow in unsaturated fractured rock–A review, in *Flow and Transport through Unsaturated Fractured Rock, Geophys. Monogr. Ser*., *42*, D. Evans and T. Nicholson, eds., pp. 11–21, AGU, Washington, DC.

Pruess, K., J.S.Y. Wang, and Y.W. Tsang (1990a), On thermohydrological conditions near high-level nuclear wastes emplaced in partially saturated fractured tuff—1. Simulation studies with explicit consideration of fracture effects, *Water Resour. Res., 26(6),* 1235–1248.

Pruess, K., J.S.Y. Wang, and Y.W. Tsang (1990b), On thermohydrological conditions near high-level nuclear wastes emplaced in partially saturated fractured tuff—2. Effective continuum approximations, *Water Resour. Res., 26(6)*, 1249–1261.

Pruess, K., and Y. Tsang (1994), Thermal modeling for a potential high-level nuclear waste repository at Yucca Mountain, *Technical Rep. LBL-35381*, Lawrence Berkeley National Laboratory, Berkeley, CA

Pruess, K., C. Oldenburg and G. Moridis (1999), TOUGH2 user's guide, Version 2.0, *Technical Report LBNL-43134*, Lawrence Berkeley National Laboratory, Berkeley, CA.

Ramirez, A. L., T. Buscheck , R. Carlson, W. Daily, K. Lee, W. Lin, N. Mao, , T. Ueng, H. Wang, and D. Watwood ((1991), Prototype Engineering Barrier System Field Test (PEBSFT) Final Report. *UCRL-ID-106159*, Lawrence Livermore National Laboratory, Livermore CA.

Rejeb, A., G. Vouille, J.C. Gros (1993), Study of the thermal and mechanical behavior of granite applied to the nuclear waste repository, conclusions drawn from the Fanay-Augères experiment. Safewaste' 93: Le devenir des dèchets nuclèaires. *Proceedings of the International conference – SFEN – Avignon 13-18/06/1993. Volume 3*: Poster Sessions, pp. 174-186.

Robinson, R. A. (1985), Summary results and conclusions from the cooperative project at Stripa, between Sweden and the United States during 1977-1980. In *Proceedings from Second NEA/SKB Symp., International Stripa Project,* (organized by OECD/NEA), Stockholm, Sweden.

Rutqvist, J., D. Barr, R. Datta, , A. Gens, , A. Millard, , S., Olivella, C.-F. Tsang and. Y. Tsang (2005), Coupled Thermal-hydrological-mechanical analyses of the Yucca Mountain Drift Scale Test – Comparison of field measurements to predictions of four different numerical models" *Int. J. of Rock Mechanics and Mining Sciences, v. 42*, p. 680-697.

Rutqvist, J. and C. F. Tsang (2003), TOUGH-FLAC: a numerical simulator for analysis of coupled thermal–hydrologic–mechanical processes in fractured and porous geological media under multi-phase flow conditions, *Proceedings of the TOUGH symposium 2003*, May 12–14, 2003, Lawrence Berkeley National Laboratory, Berkeley, CA.

Rutqvist, J., C.-F. Tsang, and Y. Tsang (2004), Analysis of stress and moisture induced changes in fractured rock permeability at the Yucca Mountain Drift Scale test, Elsevier Geo-Engineering Book Series Volume 2 *Coupled Thermo-Hydro-Mechanical-Chemical Processes in Geo-Systems*, 161-166, ed. Ove Stephansson, John A. Hudson and Lanru Jing.

Rutqvist, J., Y.S. Wu, C.F. Tsang, and G. Bodvarsson (2002), A modeling approach for analysis of coupled multiphase fluid flow, heat transfer, and deformation in fractured porous rock *International Journal of Rock Mechanics and Mining Sciences,*, v. 39, p. 429–42.

Scheidegger, A.E. (1974), *The Physics of Flow Through Porous Media*, 3rd ed., University of Toronto Press, Toronto, Ont.

Sonnenthal, E.L., C.F. Ahlers, and G.S. Bodvarsson (1997), Fracture and fault properties for the UZ site-scale flow model, Chapter 7 in "The Site-Scale Unsaturated Zone Model of Yucca Mountain, Nevada, for the Viability Assessment, *Report LBNL-40376*, Lawrence Berkeley National Laboratory, Berkeley, CA.

Sonnenthal E., A. Ito, N. Spycher, M. Yui, J. Apps, Y. Sugita, M. Conrad and S. Kawakami (2005), Approaches to Modeling Coupled Thermal, Hydrological, and Chemical Processes in the Drift Scale Heater Test at Yucca Mountain, *International Journal of Rock Mechanics and Mining Sciences, v. 42, p.* 698-719.

Spycher, N.F., E.L. Sonnenthal, and J.A. Apps (2003), "Fluid Flow and Reactive Transport Around Potential Nuclear Waste Emplacement Tunnels at Yucca Mountain, Nevada." *Journal of Contaminant Hydrology, v. 62-63, p.* 653-673.

St. John., C. M. (1985), Thermal analysis of spent fuel disposal in vertical emplacement boreholes in a welded tuff repository, *Rep. SAND84-7207*, Sandia National Laboratories, Albuquerque, NM, November.

Travis, B.J., A.H. Davis, T. D. Kunkel, and R.G. Deupree (1985), KRAK—A computer program for two-phase, two-component porous flow and fracture propagation, Rep. LA-9703, Los Alamos National Laboratory, Los Alamos, NM, April.

Tsang, C.F. (1987), Coupled processes associated with nuclear waste repositories, edited by Chin-Fu Tsang, Academic Press, San Diego,

Tsang, Y.W., J. Apps, J.T. Birkholzer, B. Freifeld, M.Q. Hu, J. Peterson, E. Sonnenthal, and N. Spycher (1999), Yucca Mountain Single Heater Test Final Report, *Technical Report LBNL-42537*, Lawrence Berkeley National Laboratory Berkeley, CA.

Tsang, Y. W. and J. T. Birkholzer (1999), Predictions and observations of the thermal-hydrological conditions in the Single Heater Test, *J. of Contam. Hydrol 38*, 385-425.

Tsang, Y.W., and K. Pruess (1987), A study of thermally induced convection near a high level nuclear waste repository in partially saturated fractured tuff, *Water Resour. Res.(23), No. 10,* pp.1958-1966.

Tsang, Y.W., and K. Pruess (1989), Preliminary studies of gas-phase flow effects and moisture migration at Yucca Mountain, Nevada, *Report LBL-28819*, Lawrence Berkeley National Laboratory, Berkeley, CA.

Tsang, Y.W., and K. Pruess (1990), Further modeling studies of gas movement and moisture migration at Yucca Mountain, Nevada, *Report LBL-29127*, Lawrence Berkeley National Laboratory, Berkeley, CA.

Tsang, Y.W., K. Pruess, and J. S. Y. Wang (1993), The role of fault zone in affecting multiphase flow at Yucca Mountain, Report LBL-33661, Lawrence Berkeley Laboratory, Berkeley, California; *Proceedings of the Fourth International Conference HLRWM*, *1*, pp. 660–666.

Van Genuchten, M. Th. (1980), A closed-form equation for predicting the hydraulic conductivity of unsaturated soil*, Soil Sci. Soc. Am. J., 44*, 892-898.

Von Konynenburg, R.A., C. F. Smith, H.W. Culham, and H. D. Smith (1986), Carbon-14 in waste packages for spent fuel in a tuff repository, *UCRL REP. 94708*, Lawrence Livermore National Laboratory, Livermore, CA.

Von Konynenburg, R.A., C.F. Smith, H.W. Culh and C.H. Otto, Jr. (1985), Behavior of carbon-14 in waste packages for spent fuel in a repository in tuff, in *Scientific Basis for Nuclear Waste Management*, *8*, C.M. Jantzen et al., eds., Material Research Society, Pittsburgh, PA..

Warren, J.E., and P.J. Root (1963), The behavior of naturally fractured reservoirs, *Soc. Pet. Eng. J., 3*, 245–255.

Wilder, D. G., and J. L. Yow (1987), Geomechanics of the spent-fuel test-Climax *Report UCRL-53767*, Lawrence Livermore National Laboratory, Livermore, CA.

Wilder, D.G., W. Lin, S.C. Blair, T.A. Buscheck, R.C. Carlson, K. Lee, and A. Meike (1998), Large Block Test status report, *Tech. Rep.USRL-ID-128776*, Lawrence Livermore National Laboratory, Livermore, CA.

Witherspoon, P.A. (2000), The Stripa Project, *Int. J. Rock Mech. Min. Sci.* 37, 385.

Wu, Y. S., C. F. Ahler, P. Frazer, A. Simmons, K. Pruess (1996), Software qualification of selected TOUGH2 modules, *Rep. LBL-39490*, Lawrence Berkeley National Laboratory, Berkeley, CA.

Wu, Y-S., C. Haukwa, and G.S. Bodvarsson (1999), A site-scale model for fluid and heat flow in the unsaturated zone of Yucca Mountain, Nevada, *Journal of Contaminant Hydrology, v. 38,* (1-3), p. 185-215.

Wu, Y-S., L Pan, W. Zhang, and G.S. Bodvarsson (2002), Characterization of flow and transport processes within the unsaturated Zone of Yucca Mountain, Nevada, Under Current and Future Climates, *Journal of Contaminant Hydrology, v. 54,* (3-4), p. 215-247.

Xu, T.; E. Sonnenthal, N. Spycher, K. Pruess, G. Brimhall, and J. Apps (2001), Modeling Multiphase Non-Isothermal Fluid Flow and Reactive Geochemical Transport in Variably Saturated Fractured Rocks: 2. Applications to Supergene Copper Enrichment and Hydrothermal Flows, *American Journal of Science, v. 301,* (1), p. 34-59.

Xu, T., E. Sonnenthal, N. Spycher, and K. Pruess (2004)*, TOUGHREACT User's Guide: A simulation Program for Non-isothermal Multiphase Reactive Geochemical Transport in Variably Saturated Geologic Media, Technical Report LBNL-55460*, Ernest Orlando Lawrence Berkeley National Laboratory, Berkeley, California.

Xu, T., E. Sonnenthal, N. Spycher, and K. Pruess (2006), TOUGHREACT: A simulation program for non-isothermal multiphase reactive geochemical transport in variably saturated geologic media. LBNL-56740. *Computer & Geosciences, 32 (2*), 145–165, 2006.

Zimmerman, R. M., M. L. Blanford, J. F. Holland, R.L Schuch, and W. H. Barrertt (1986a), Final Report: G-Tunnel Small-Diameter Heater Experiments. *SAND84-2621,* Sandia National Laboratories, Albuquerque, NM.

Zimmerman, R. M., R.L. Schuch, D.S. Mason, M. L. Wilson, M. E. Hall, M. P. Board, R. P. Bellman, and M. L. Blanford (1986b), Final Report: G-Tunnel Heated Block Experiments. *SAND84-2620*, Sandia National Laboratories , Albuquerque, NM.

FIGURE CAPTIONS

Figure 1. Schematic of thermal-hydrological coupled processes in fractured welded tuff

Figure 2. Idealized waste container emplacement configuration. An infinite linear string of waste containers is intersected by fractures with 0.22 m spacing

Figure 3. Schematic of a borehole layout in the Single Heater Test (schematic 3-D perspective, plan view and cross section). The numbers in the cross section denote borehole identity

Figure 4. Conduction-only and full thermal-hydrological simulations compared with Single Heater Test temperature data at 9 months of heating. For the X axis, origin is at the heater hole 1

Figure 5. Simulated fracture liquid saturation at 3 months and 9 months of heating, and 3 months of cooling; in Single Heater Test XZ–cross section at Y = 4.5 m, mid-plane of the Heater hole 1

Figure 6. Air-permeability measurements in Zone 3 of boreholes 16 and 18 for before, during, and after heating phase of the Single Heater Test

Figure 7(a). Three-dimensional perspective of heaters and boreholes in the Drift Scale Test; (b) temperature boreholes configuration in the Drift Scale Test; and (c) electric resistivity tomography and neutron/ground penetrating radar boreholes configuration in the Drift Scale Test

Figure 8. Measured (top) and simulated (bottom) temperature profiles along the eight Drift Scale Test boreholes, 158 to 165, at 3 months of heating

Figure 9. Measured (top) and simulated (bottom) temperature profiles along the eight Drift Scale Test boreholes 158 to 165, at 18 months of heating

Figure 10. Temperature history of selected sensors in Drift Scale Test borehole 160

Figure 11. Change in matrix saturation from preheat saturation: (a) measured ground penetrating radar data in Drift Scale Test boreholes 49-51 in January 2002 (near the end of heating) and (b) simulated results at end of heating phase

Figure 12. Drying in Drift Scale Test from electric resistivity tomography and neutron logging data, and simulated contour of matrix liquid saturation of 50% (preheat ambient matrix liquid saturation is above 90%)

Figure 13. Schematic representation of the test block in the Large Block Test (not to scale)

Figure 14. Comparison of measured and simulated temperatures (with discrete fractures embedded in a dual permeability model) at selected sensor locations of Large Block Test borehole TT1 immediately before and after the rain event, which initiated at 4470 hours of heating

Figure 15. Comparison of measured and simulated temperatures (with a discrete fracture embedded in a dual-permeability model) at selected sensor locations of Large Block Test borehole TT2 immediately before and after the rain event, which initiated at 4470 hours.of heating

Figure 16. Schematic diagram showing the thermal, hydrologic, and chemical processes at the fracture-matrix interface (matrix to the back, and fracture to the front)

TABLES

Table 1. Thermal and hydrological processes in strongly heat-driven flow in partially saturated rock

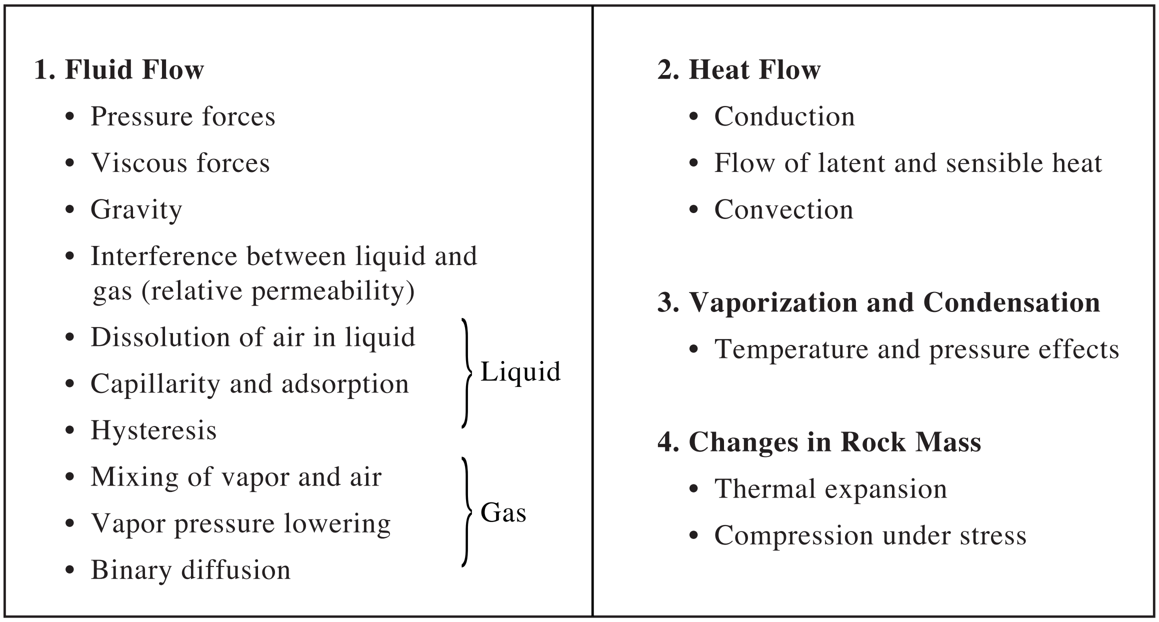

1. Fluid Flow

- Pressure forces
- Viscous forces
- Gravity
- Interference between liquid and gas (relative permeability)
- Dissolution of air in liquid
- Capillarity and adsorption
- Hysteresis

Liquid

- Mixing of vapor and air
- Vapor pressure lowering
- Binary diffusion

Gas

2. Heat Flow

- Conduction
- Flow of latent and sensible heat
- Convection

3. Vaporization and Condensation

- Temperature and pressure effects

4. Changes in Rock Mass

- Thermal expansion
- Compression under stress

Table1_YTsangAGU_bw.eps

Table 2. Coupling of thermal, hydrological, and mechanical processes. The diagonal elements contain the “fundamental” parameters of each respective process. Each off-diagonal element indicates how the “row” process impacts the parameter in the “column” process.

	Thermal	**Hydrological**	**Mechanical**
Thermal	Temperature Heat flux	Fluid density Viscosity	Thermal expansion
Hydrological	Heat convection Thermal conduction Specific heat	Fluid flow Pressure	Effective stress Moisture Swelling
Mechanical	N/A, see text	Porosity Permeability	Stress Strain

Figure 1. Schematic of thermal-hydrological coupled processes in fractured welded tuff

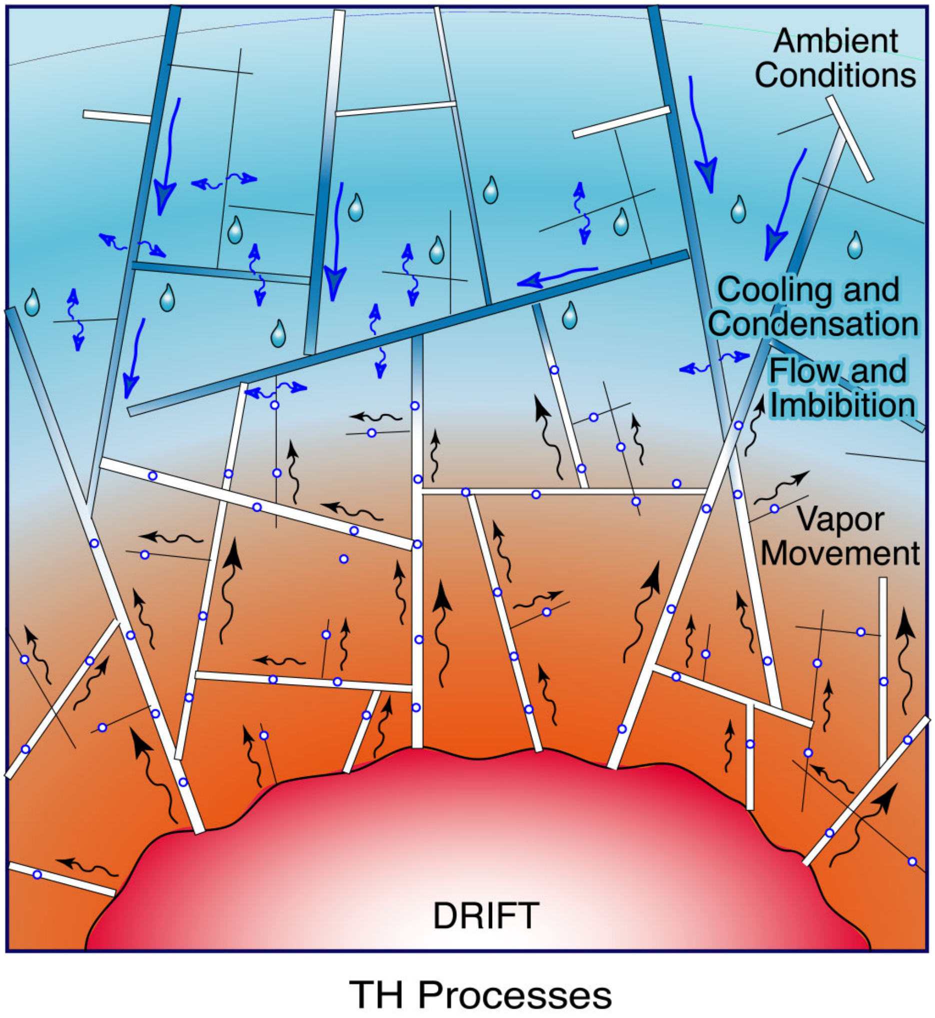

Figure 2. Idealized waste container emplacement configuration. An infinite linear string of waste containers is intersected by fractures with 0.22-m spacing.

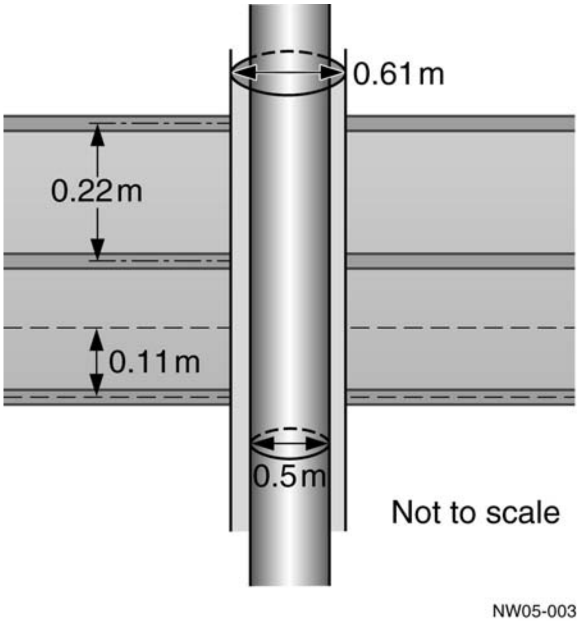

Figure 3. Schematic of borehole layout in the Single Heater Test (3-D perspective and cross-section). The numbers in the cross section denote borehole identity.

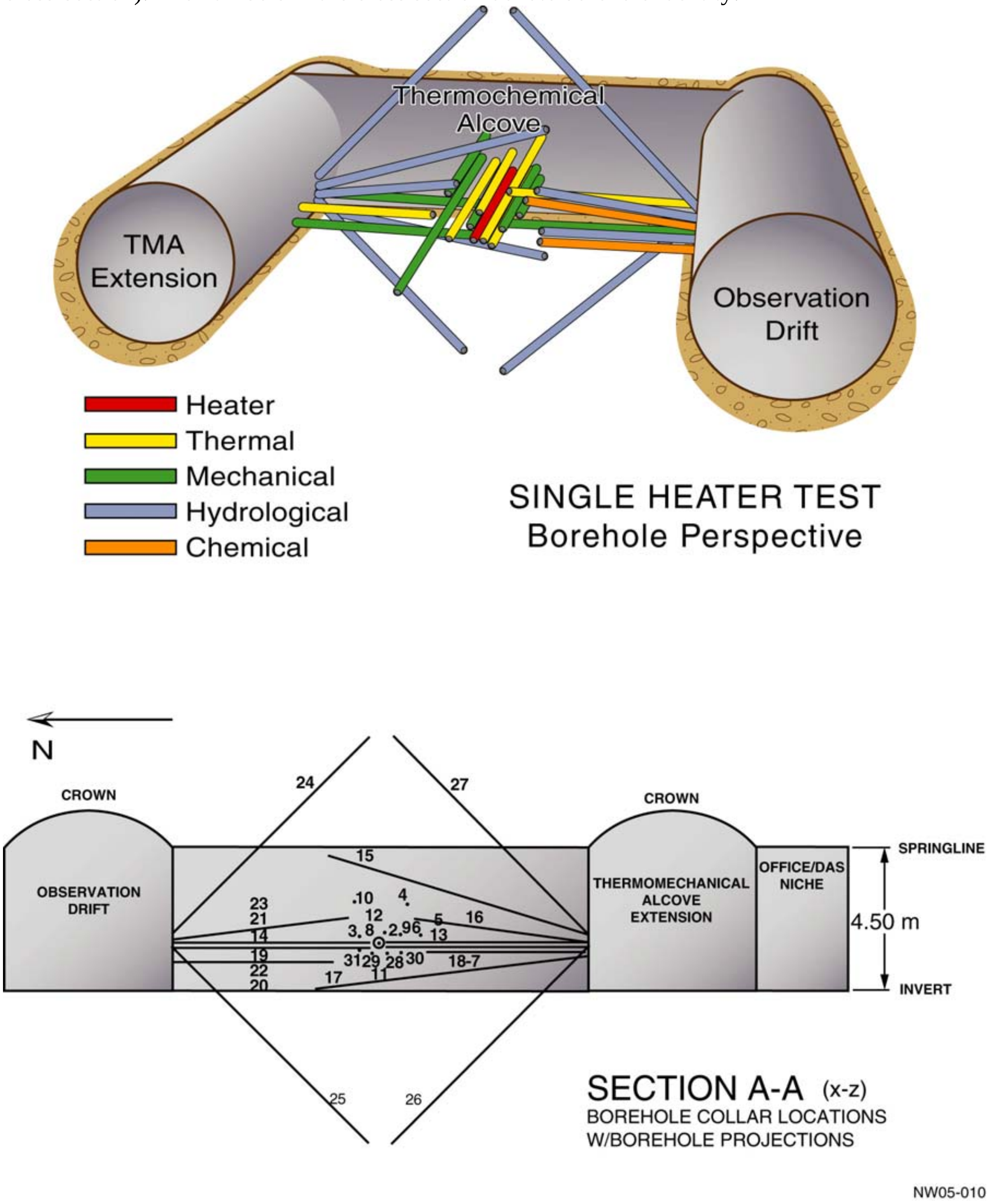

Figure 4. Conduction only and full TH simulations compared with Single Heater Test temperature data at 9 months of heating. For the X axis, origin is at the heater hole 1.

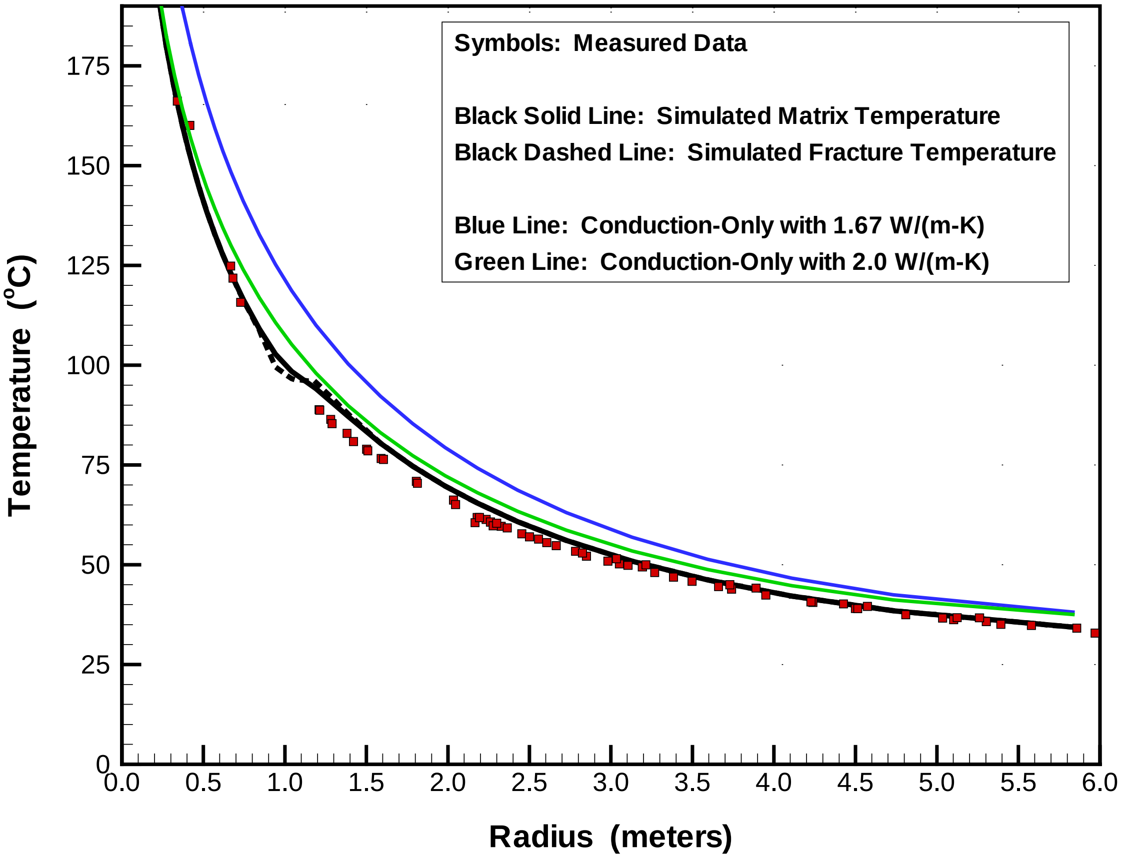

Figure 5. Fracture liquid saturation at 3 months, 9 months of heating, and at 3 months of cooling

Figure 5a. Simulated fracture liquid saturation after 3 months of heating in X-Z section at Y = 4.5 m , mid-plane of the Heater Hole 1

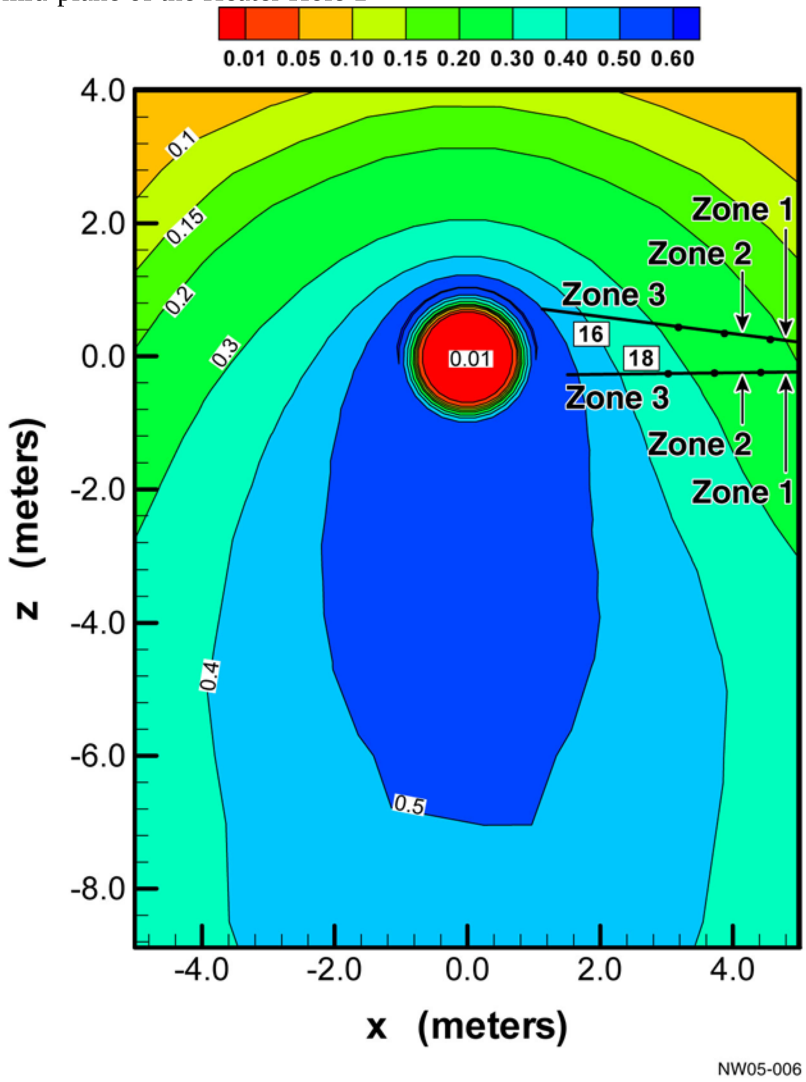

Figure 5b. Simulated fracture liquid saturation after 9 months of heating in X-Z section at Y = 4.5 m, mid-plane of the Heater Hole 1.

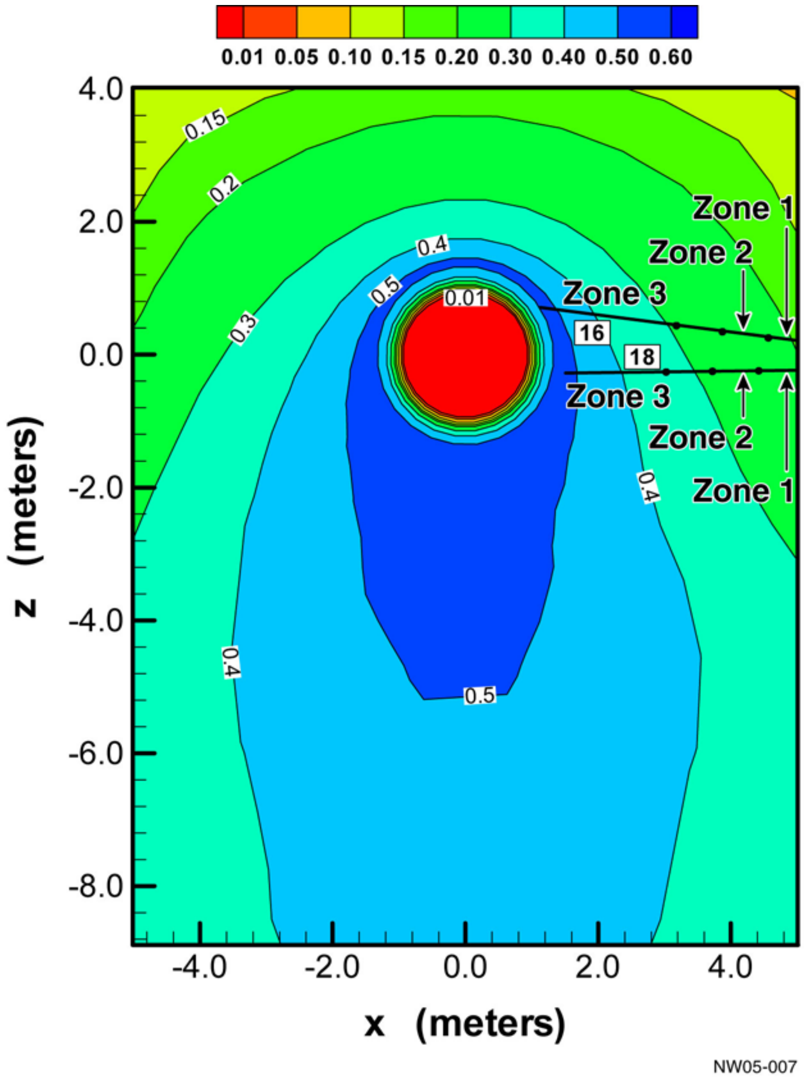

Figure 5c. Simulated fracture liquid saturation after 3 months of cooling in X-Z section at Y = 4.5 m, mid-plane of the Heater Hole 1

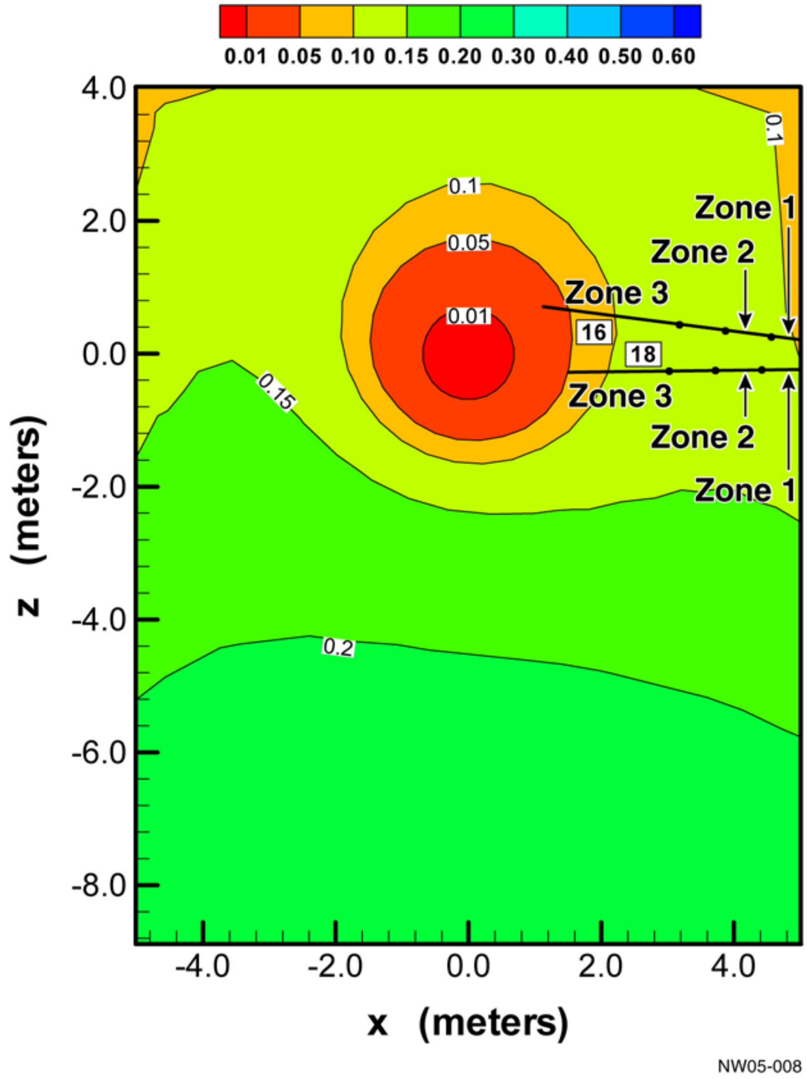

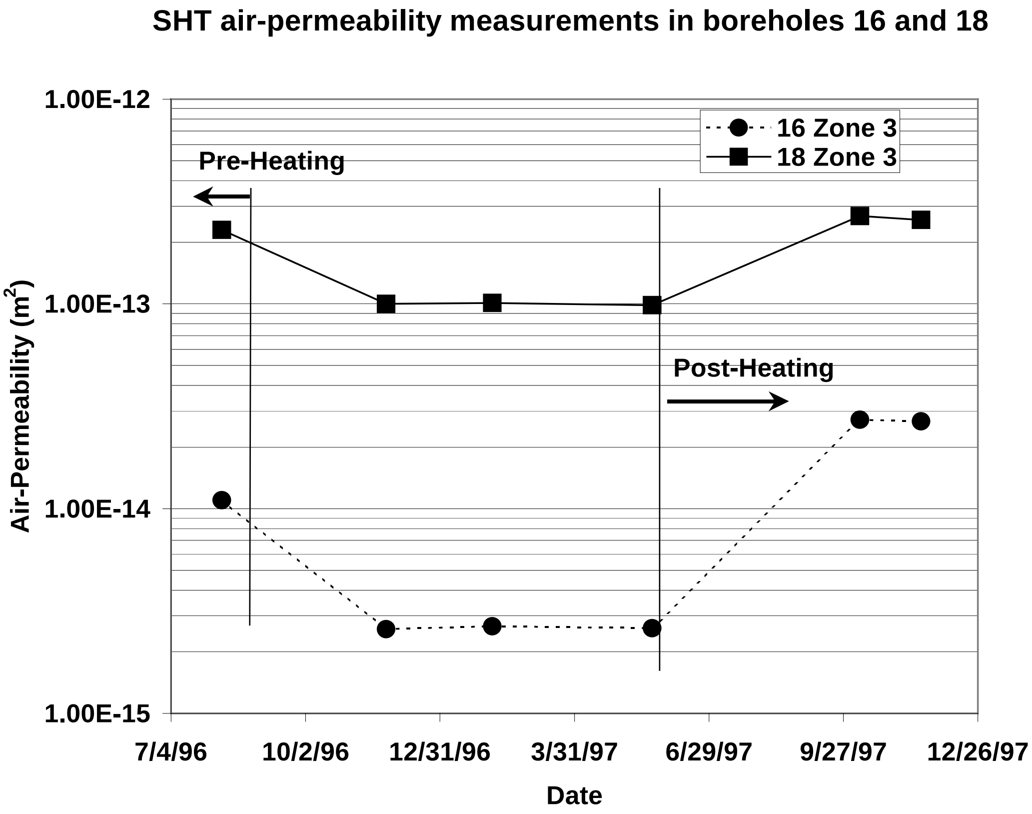

Figure 6. Air-permeability measurements in Zone 3 of boreholes 16 and 18 for before, during, and after heating phase of the Single Heater Test.

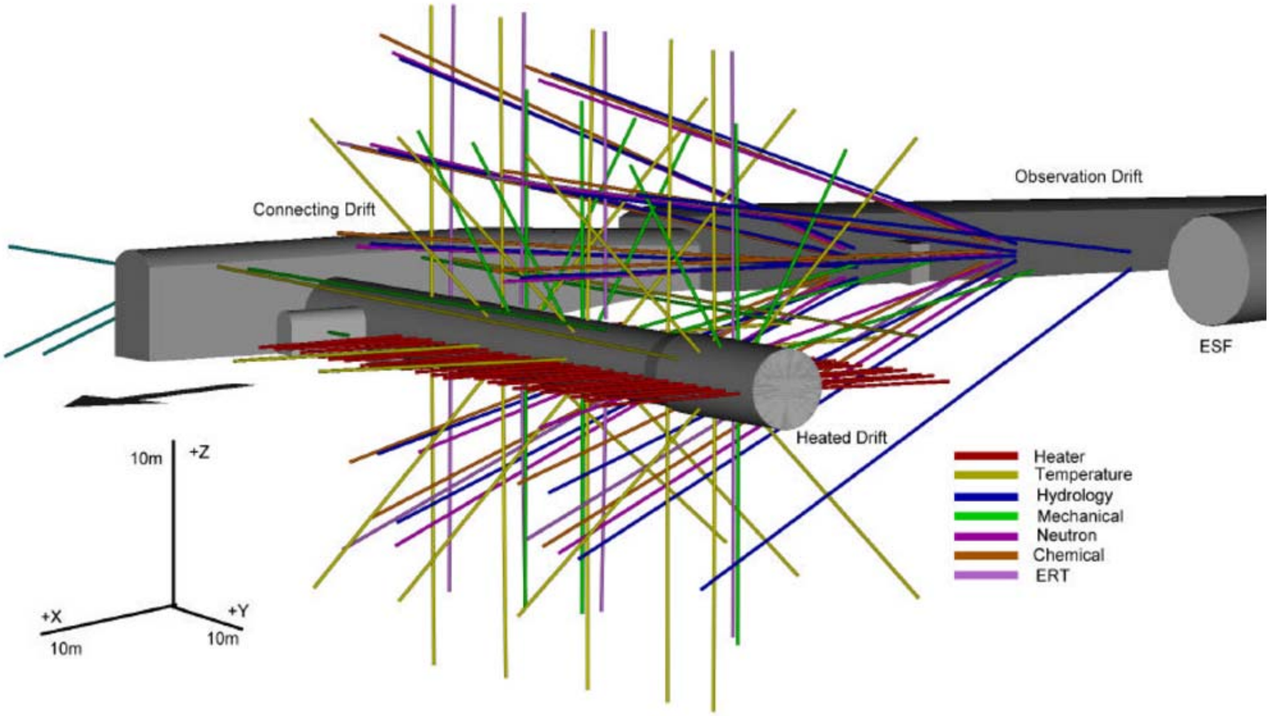

Figure A-1. Perspective View Showing Drifts and Boreholes of the Drift Scale Test.

Figure 7a. 3D perspective of heaters and boreholes in the Drift Scale Test

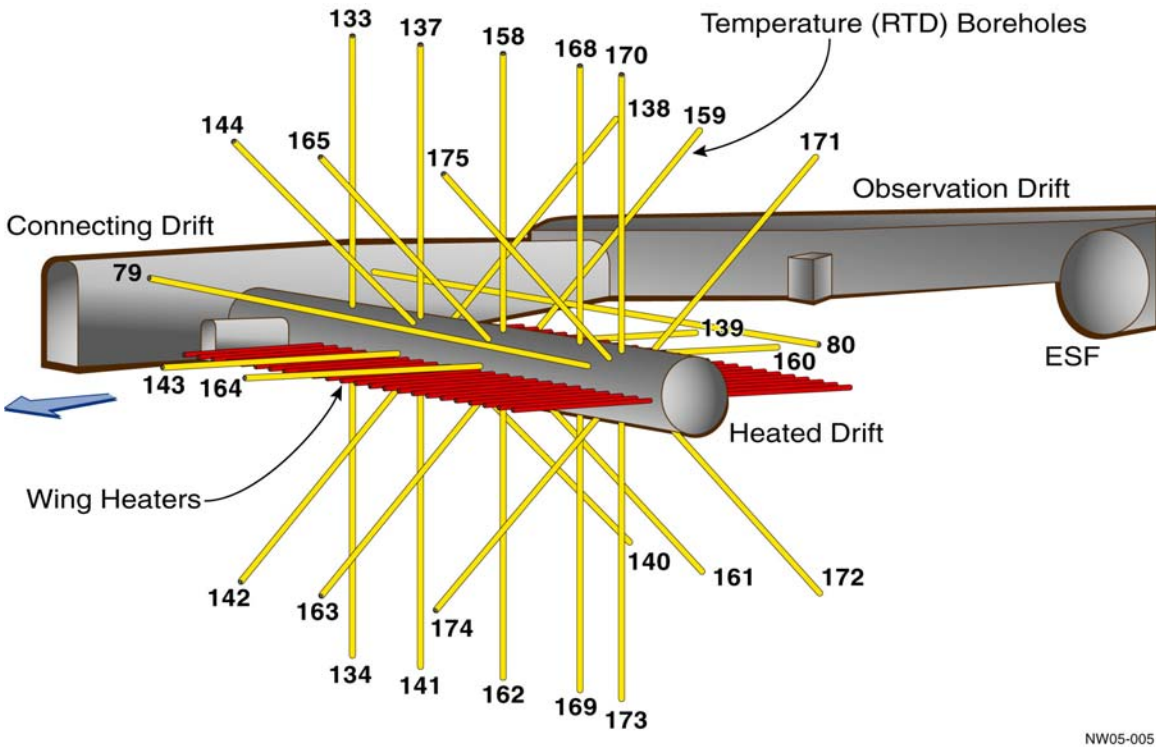

Figure 7b. Temperature boreholes configuration in the Drift Scale Test

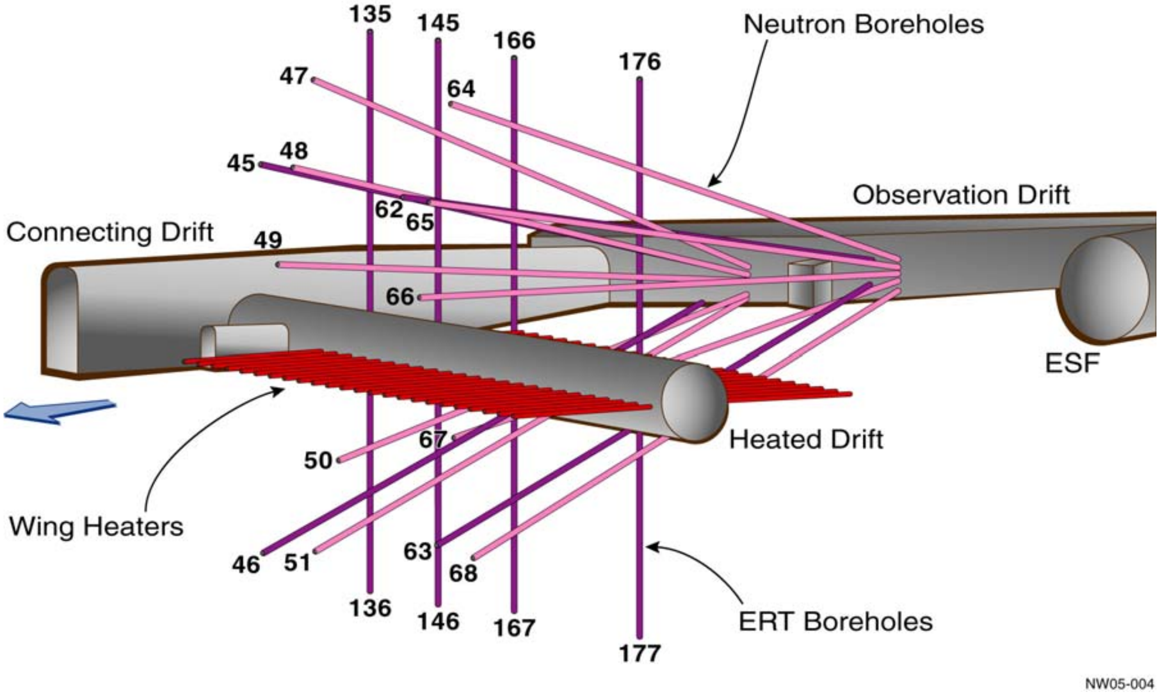

Figure 7c. Electric resistivity tomography and neutron/ground penetrating radar borehole configuration in the Drift Scale Test

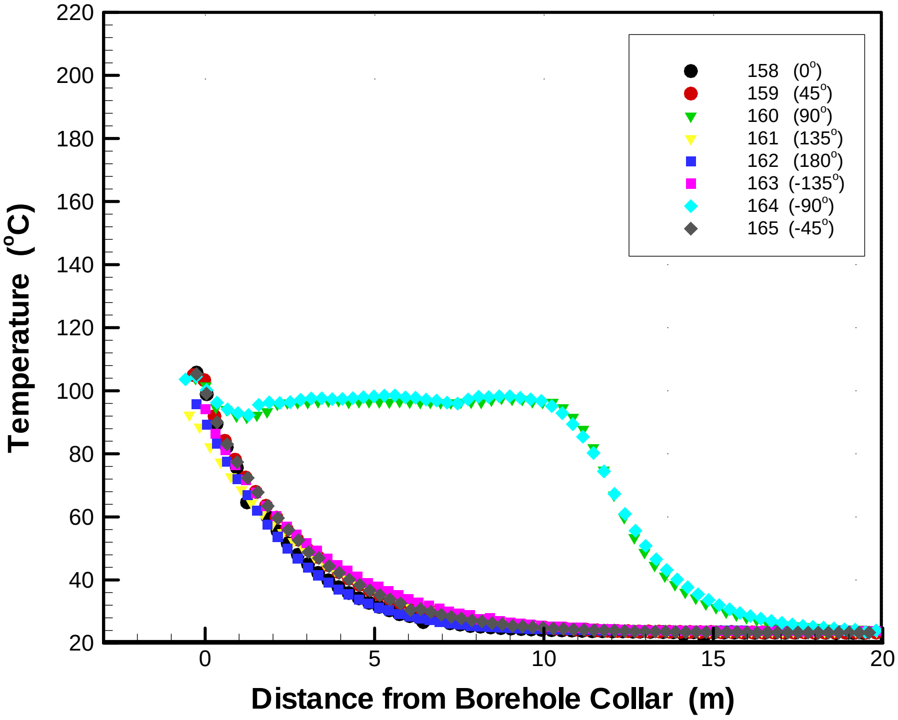

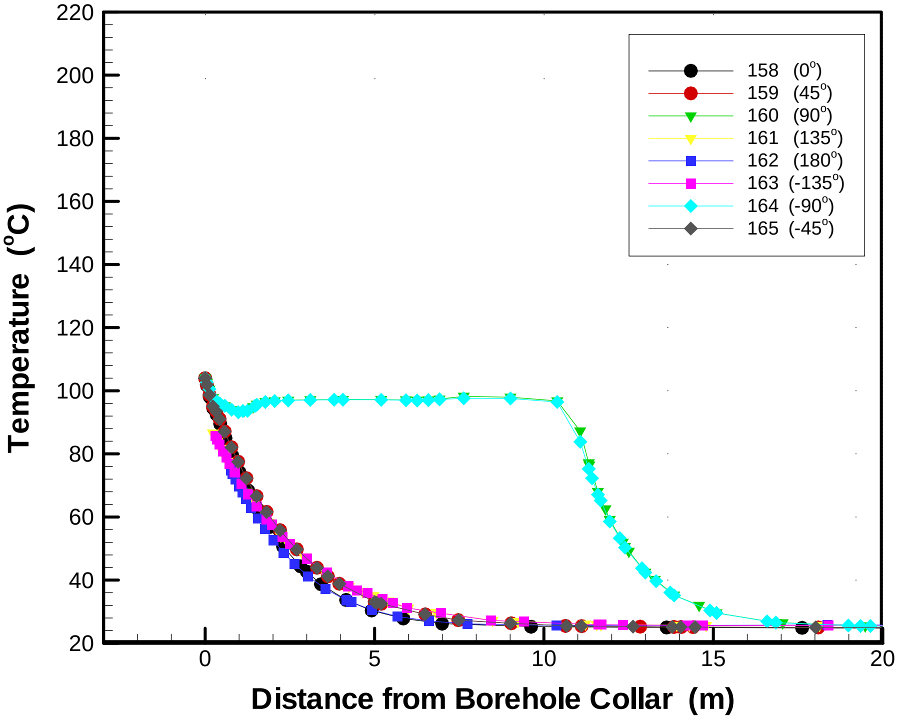

Figure 8. Measured (top) and simulated (bottom) temperature profiles along the eight Drift Scale Test boreholes, 158 to 165, at 3 months of heating

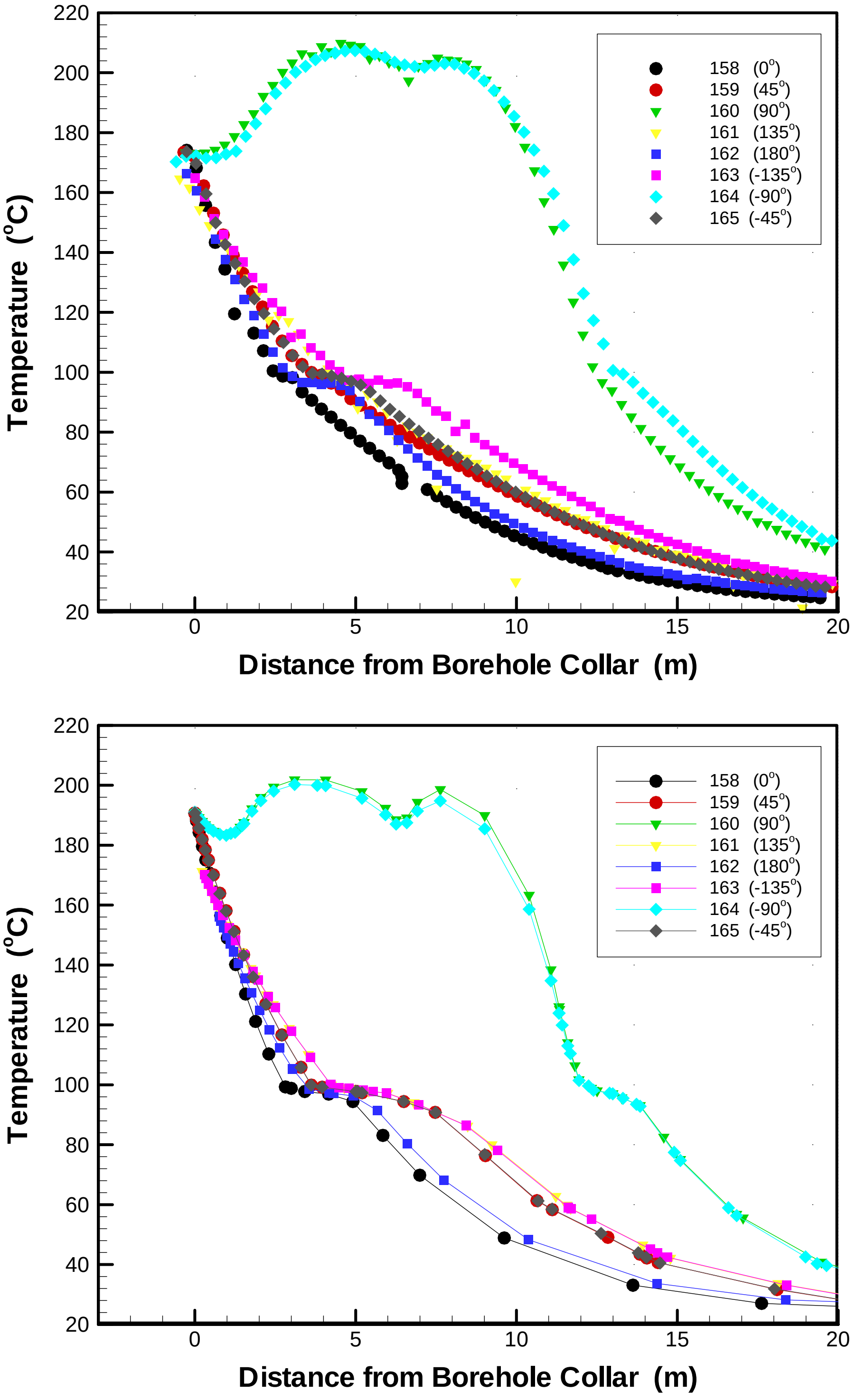

Figure 9. Measured (top) and simulated (bottom) temperature profiles along the eight Drift Scale Test boreholes 158 to 165, at 18 months of heating

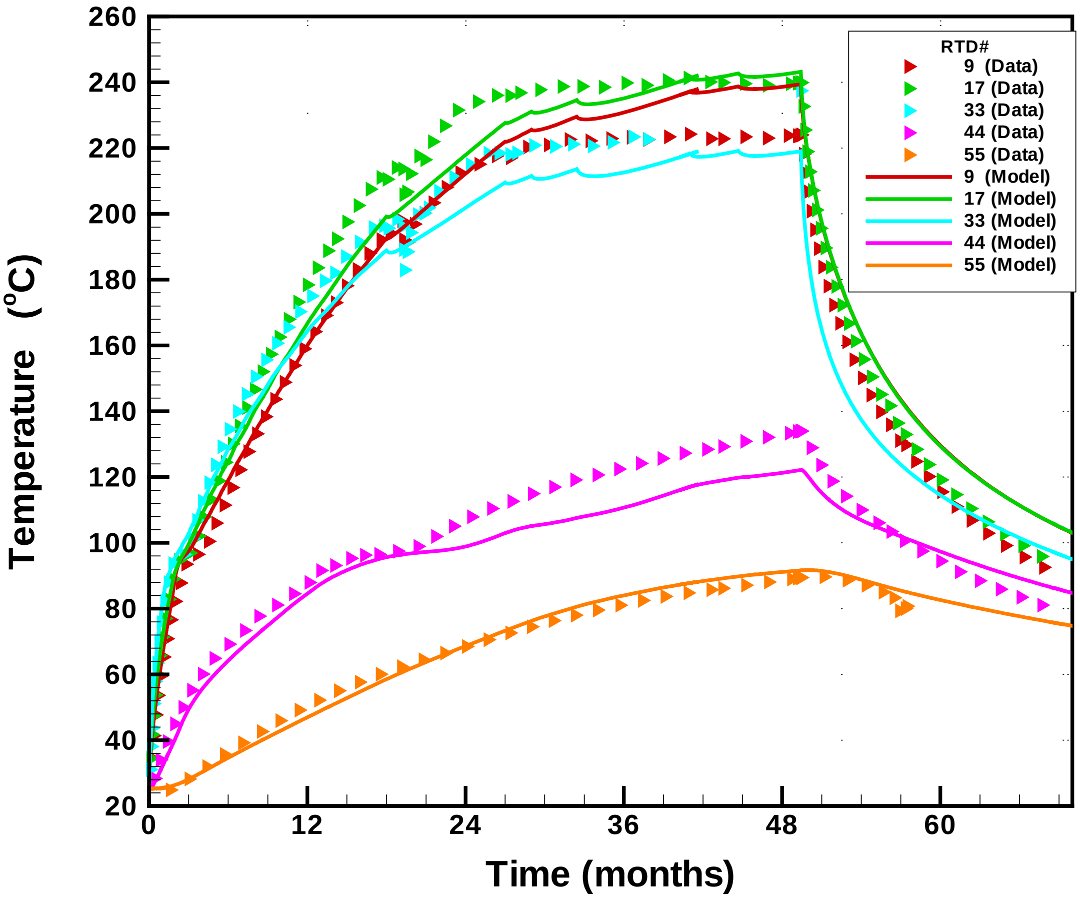

Figure 10. Temperature history of selected sensors in Drift ScaleTest borehole 160

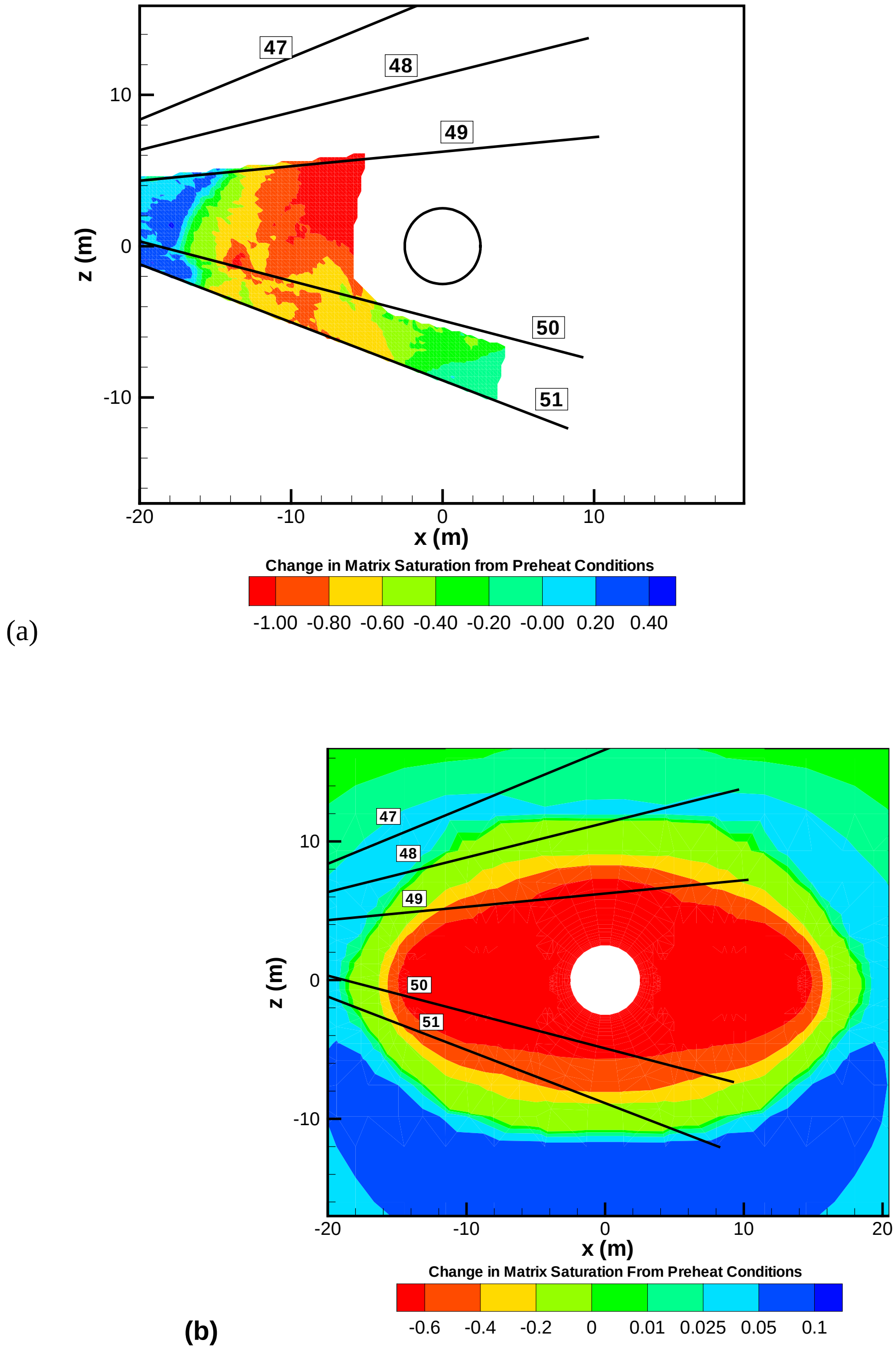

Figure 11. Change in matrix saturation from preheat saturation: (a) measured ground penetrating radar data in the Drift Scale Test boreholes 49-51 in January 2002 (near the end of heating) and (b) simulated results at end of heating phase

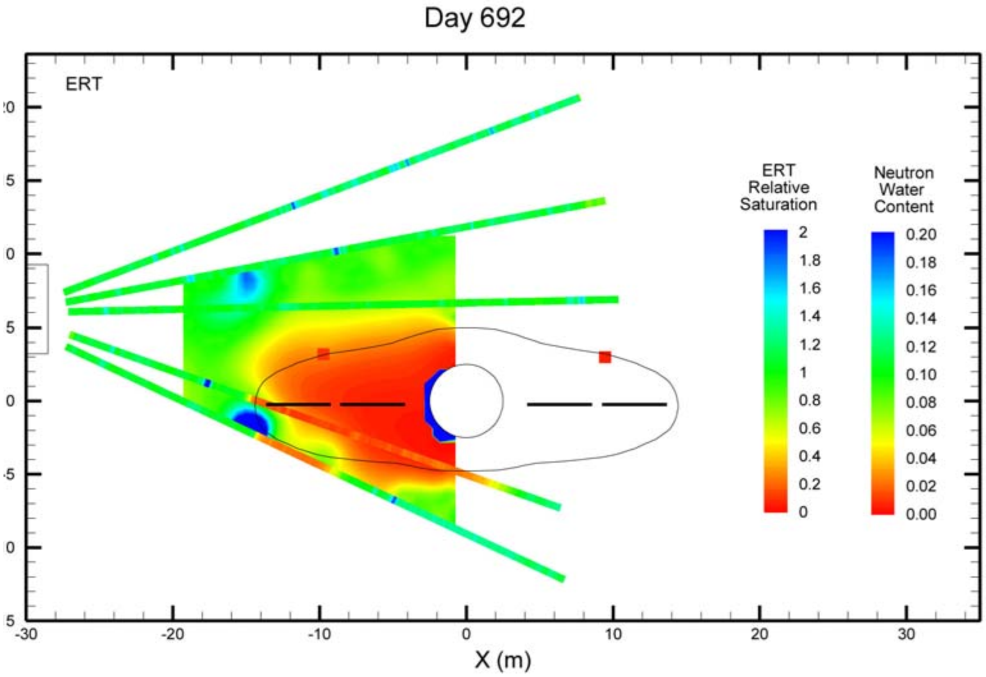

Figure 12. Drying in the Drift Scale Test from electric resistivity tomography and neutron logging, and simulated contour of matrix liquid saturation of 50% (preheat ambient matrix liquid saturation is above 90%)

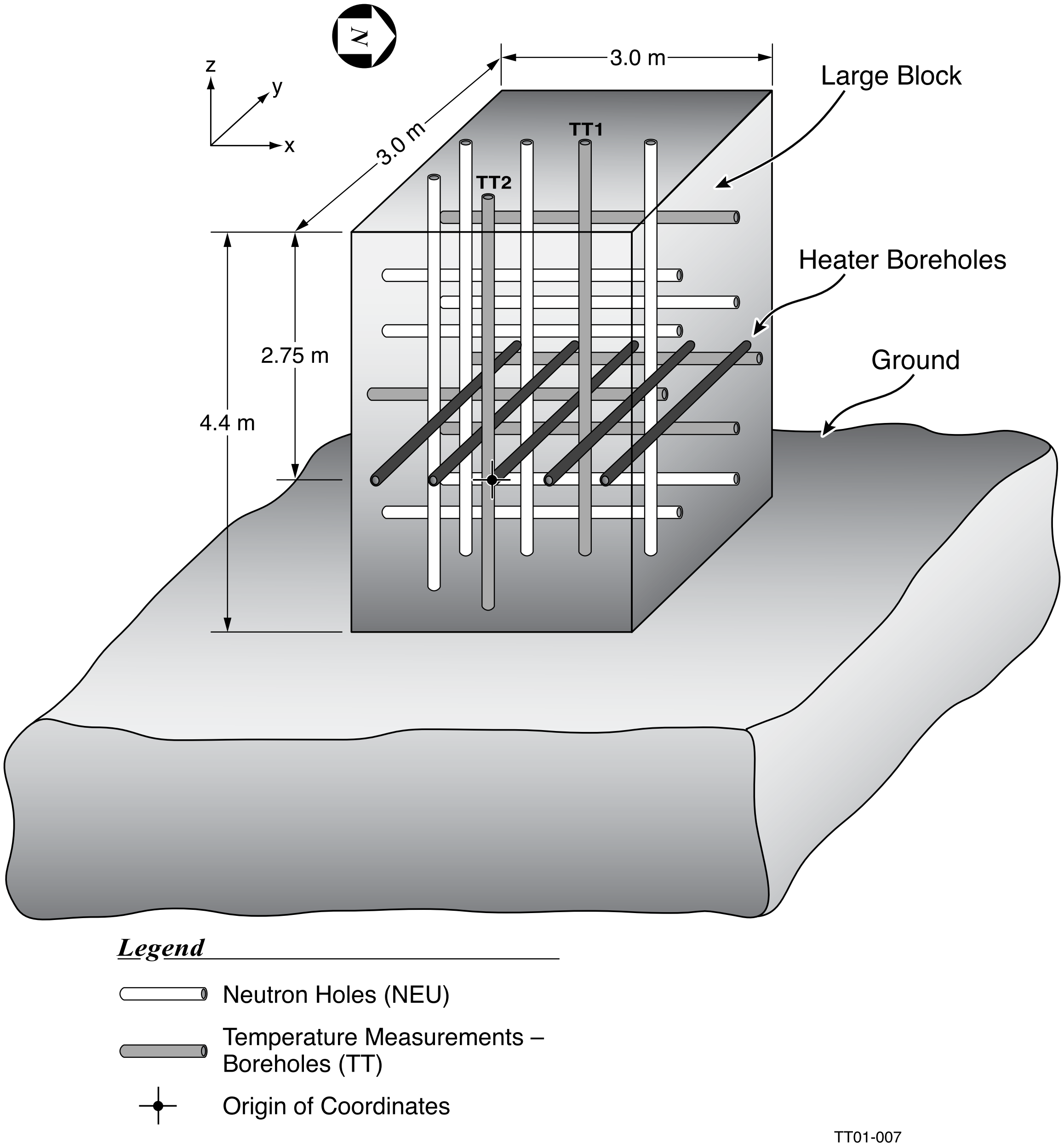

Figure 13. Schematic representation of the test block in the Large Block Test (not to scale)

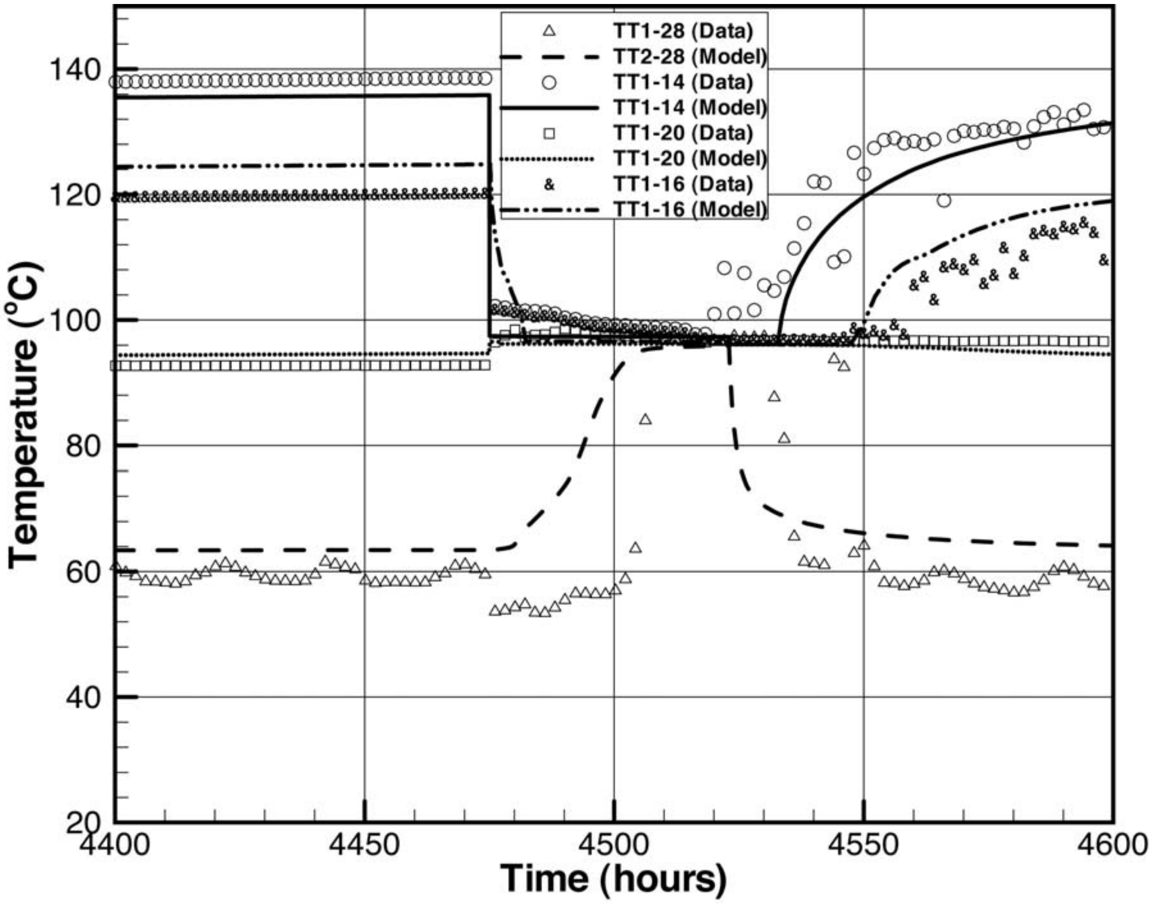

Figure 14. Comparison of measured and simulated (with discrete fractures embedded in a dual-permeability model) temperatures at selected sensor locations of Large Block Test borehole TT1 immediately before and after the rain event, which initiated at 4470 days of heating.

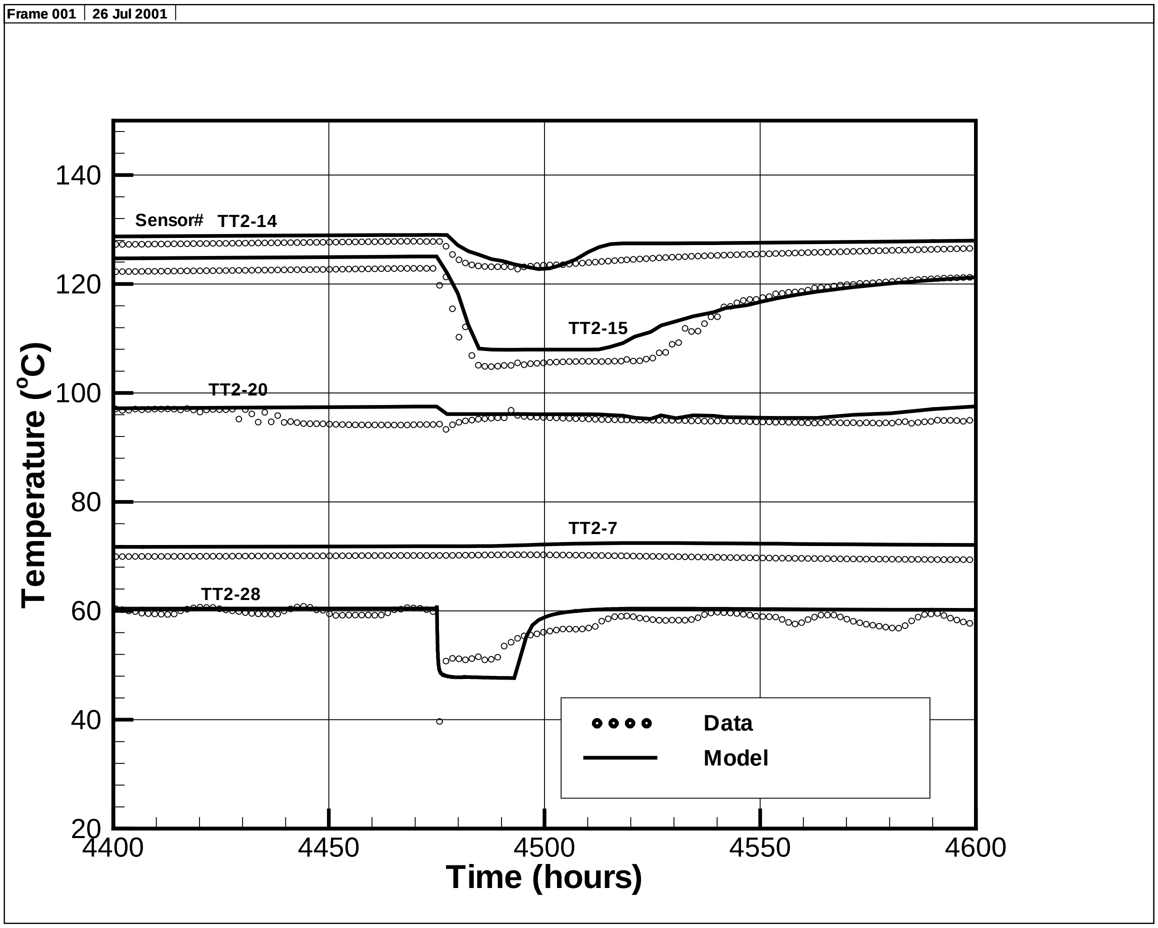

Figure 15. Comparison of measured and simulated (with a discrete fracture embedded in a dual-permeability model) temperatures at selected sensor locations of Large Block Test borehole TT2 immediately before and after the rain event, which initiated at 4470 hours of heating.

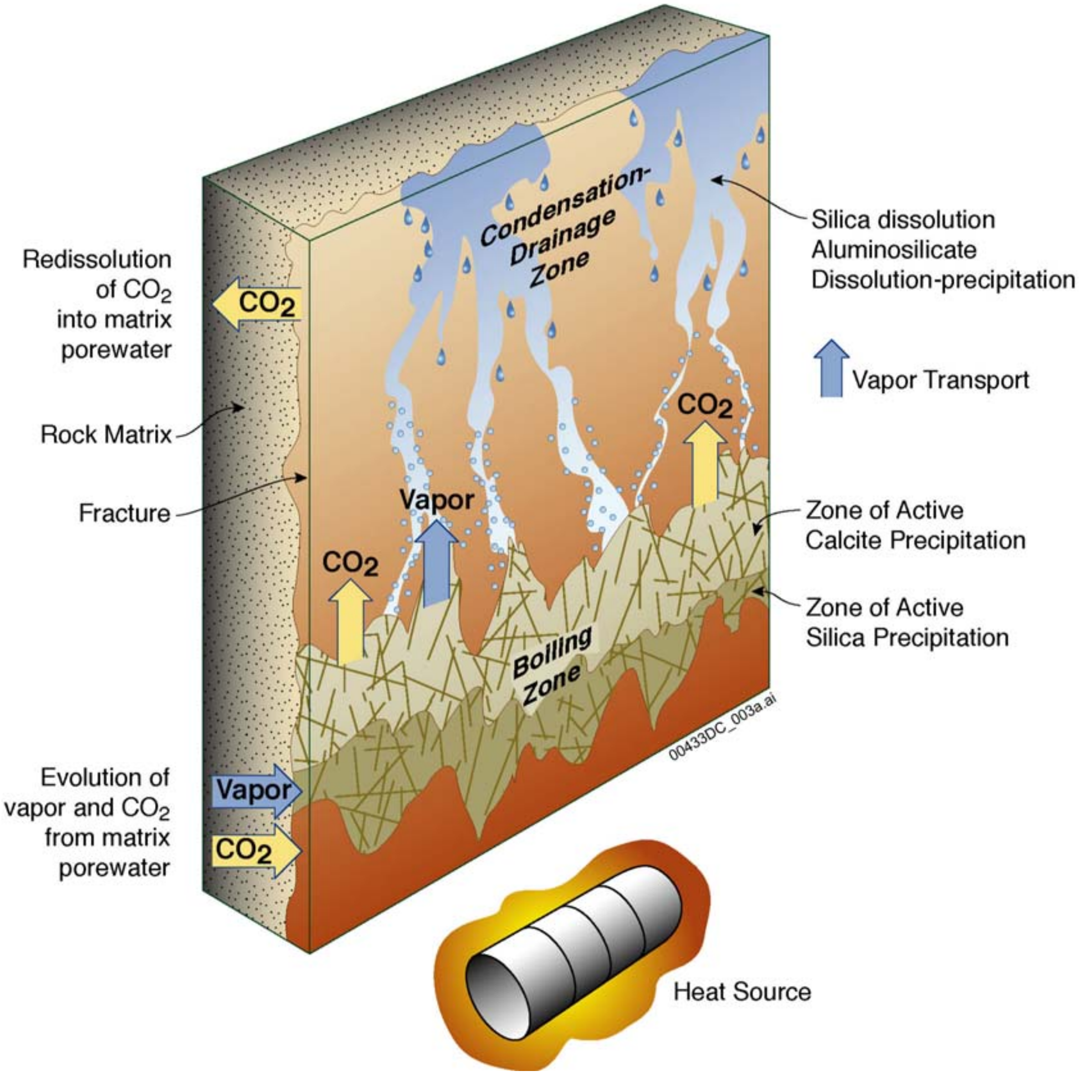

Figure 16. Schematic diagram showing the thermal, hydrologic, chemical (THC) processes at the fracture-matrix interface (matrix to the back, and fracture to the front)